Final Project Report

Improved understanding of the use of short tendons for stope support under rockfall and rockburst conditions (Phase I)

D.P. Roberts, M.K.C. Roberts, E. Acheampong

Research agency: CSIR Mining Technology

Project number: GAP 849

Date: March 2002

Executive Summary

The aim of this project was to determine whether the introduction of short bolts into a stope hangingwall would increase the stability of the hangingwall beam.

A simple physical 1/10th hangingwall model was constructed out of concrete, with properties scaled accordingly. The analytical theory behind the scaling procedure is outlined in this report. The hangingwall model was supported at either end, confined laterally, and loaded to destruction vertically. Simulated rockbolts were installed and a significant increase in the strength (4.6 times), stiffness (7.7 times) and energy absorbing capacity (2.5 times) was observed. The modelling procedure, setup and interpretation of results are discussed.

The scaled-down hangingwall was analysed using numerical modelling. Various quantitative similarities in the results were observed. The increase in strength and stiffness when bolts were included was much less than in laboratory models, and the reasons for these differences are discussed. Numerical modelling was employed in generating and analysing hangingwall models representing three generic hangingwall types: VCR, Vaal Reefs and Carbon Leader. Bolts were introduced into these models based on expected practice for the generic types. Increases in the hangingwall beam strength varied from 4% to 22%. The mode of failure of the beam and the positions of bolts relative to the discontinuity planes along which failure was observed was crucial towards mobilising resistance to failure. When bolts intersected discontinuities involved in failure, the beam was stronger.

The test-lab and numerical modelling procedures were evaluated and improvements to both are suggested in this report. In conclusion, the scope and focus of the next phase of this project are outlined.

Acknowledgements

Many individuals contributed towards the completion of the laboratory tests, which proved to be much more time-consuming and challenging than anticipated. Firstly, Dr. Rod Smart of FOSROC Stratabolt, was most helpful in timeously supplying the required concrete mixes. Bob Holloway of Qualitec Engineering is to be thanked for turning out the frame to spec and on time.

The test-lab staff are to be thanked for their patience and other contributions. Bruce Jack and Flippie Swart, for their helpful suggestions and expert piloting of the Terratek machine, and Sipho Mashele and Hendrik Shibodze, for helping out enthusiastically whenever possible. Davis Mabuza is thanked for his many contributions, including contingencies for plans A through G. Thanks also to Gary Prohaska and Eric Jaku for their assistance.

Table of Contents

List of Figures

List of Tables

1. Introduction

The use of rockbolt support in South African Gold Mines is well established. However, application in stopes is uncommon, and is limited to stabilisation of ground to prevent rock falls. Rockbolt support systems are not used in stopes which may be subjected to rockburst damage. Rockbolts are used primarily in two applications: reinforcement and suspension. Reinforcement increases the integrity of a discontinuous rock mass by holding adjacent blocks together and "helping the rock mass to support itself". Suspension involves tying an unstable or fractured area to a stable or intact region.

The suspension role is called for in situations where the rock is regularly bedded, as in coal mines, or where the integrity of the area is crucial, for example, near shafts. Pre-tensioned end-anchor bolts or cables are usually used for this purpose.

Reinforcement is a more complex concept. The benefit of tying adjacent rock blocks together is only realised when the discontinuity pattern, the mode of failure of the rock mass and the bolting pattern, are complementary. For example, installing bolts parallel to a single joint set will have no reinforcement effect whatsoever. The bolts must be installed so that they assist in the building of beams or arches. In most deep-level areas, bolts are used to stabilise the fractured ground around tunnel excavations. In this role the bolts are installed in a radial pattern, which, with the assistance of large confining stresses, create a reinforced arch.

In tabular excavations, the goal of support is to maintain hangingwall integrity, and the support role tends to beam building rather than arch formation. The practical limitations on bolting imposed by production and geometric constraints are such that only bolts shorter than the stoping width (typically 0.5 m to 1.5 m) can be installed in a single production cycle. While it is highly probable that bolts extending through the entire fractured region in the hangingwall will be beneficial, it is not known whether shorter bolts will contribute significantly.

The aim of this project was to answer that question: do short bolts increase the integrity and stability of the hangingwall? The means of investigation in this project were numerical and laboratory models. The lab tests focused on the basic question of whether the introduction of short bolts into one layer of a discontinuous rock mass will increases the strength, energy absorbing capacity and stiffness of the beam. The first objective of the numerical analysis was to corroborate the results of the lab tests by exactly modelling the test setup and procedure. An exhaustive literature survey was also conducted, detailing instances where bolts have been employed in stope hangingwalls. Generic hangingwall types encountered in South African gold mines were described. Numerical models of these generic types were constructed and modelled with and without bolts. The results from the analyses are comparative, that is, the bolted and unbolted case is always compared. The aim was not to quantify the strength of these beams.

This is the first phase of a research process that must ultimately quantify the strengthening effect of bolting patterns, and provide guidelines for bolt types and patterns for any given hangingwall geometry. Based on the work performed, recommendations on the direction and emphasis of this research have been included, to outline the scope and focus of the next phase of the project.

2. Literature survey

2.1. Introduction

This survey concentrates on three areas of primary interest. The first of these is the characterisation of the hangingwall. A coherent picture of typical hangingwall conditions and geometry must be built up before modelling of this environment can begin. Secondly, the mechanisms and action of reinforcing elements must be studied. The role of rockbolts and rock tendons varies from mine to mine and from site to site. This role must be identified in terms of current research, i.e. reinforcement of a fractured, bedded mine roof. Appropriate support may then be selected based on the findings. Thirdly, prior attempts to stabilise the hangingwall with rock reinforcement must be investigated. Such attempts may serve as calibration for models and may highlight dangers and unexpected effects.

2.2. Characterisation of the hangingwall

What exactly is meant by characterisation? The rock mechanics parameters defining a mine roof are the distribution and orientation of discontinuities, the nature and orientation of these discontinuities, and the properties of materials within the roof. The stress state within the roof is also crucial to predicting its behaviour. The orientation of principal stresses and their relative magnitudes define the stress state around an excavation.

Depending on the geotechnical area, the hangingwall (and footwall) in gold and platinum environments is typically stratified, usually parallel to the stope horizon. In deep-level gold mines, mining-induced fractures appear in both the hangingwall and footwall, following excavation and face advance. These fractures may be divided into different types according to the mechanism by which they were formed. Each of these types shows a consistency of orientation and regularity in the distribution of fractures. The fracture groups may therefore be fully defined by single values of orientation, spacing, length and persistence (extension into the plane). The bedding planes and fracture groups at various orientations intersect and combine to form the fragmented and blocky hangingwalls encountered underground.

This section attempts to define and identify the fracture types and their expected orientations, spacings and extents. A number of researchers have worked in this area and produced a number of meaningful and insightful publications. Their work is now discussed.

2.2.1. Deep level gold mining hangingwall conditions

One of the first investigations of observed fracture patterns around deep level stopes was conducted by Leeman (1958). He observed two types of fractures, which he termed “slabbing” failure and “ring stress” failure. The slabbing failures were closely spaced and parallel to the major principal stress direction. “Ring stress” failures were attributed to a shear mechanism. No attempt was made at characterising or quantifying the fracture interface properties. An elegant (though largely empirical) picture of fracturing around a stope was proposed and is presented in Figure 1.

Cook (1962) proved that stresses near the face were high enough to cause failure of quartzite, resulting in observed fractures in the face area. Through a series of laboratory tests it was shown that the behaviour of quartzite could be described by a Mohr-Coulomb-type model. The samples failed along “shear planes” that formed wedges, subsequently splitting the samples in tension.

Fairhurst and Cook (1966) stated that “splitting parallel to the direction of maximum compression is the principal mode of macroscopic fracture in brittle rock”. This conclusion was based on models that showed that fracture could be described by extension of cracking around Griffith flaws in a compressive stress field. This is now a well-established principle of rock mechanics and explains such phenomena as “sidewall slabbing” observed in tunnel sidewalls.

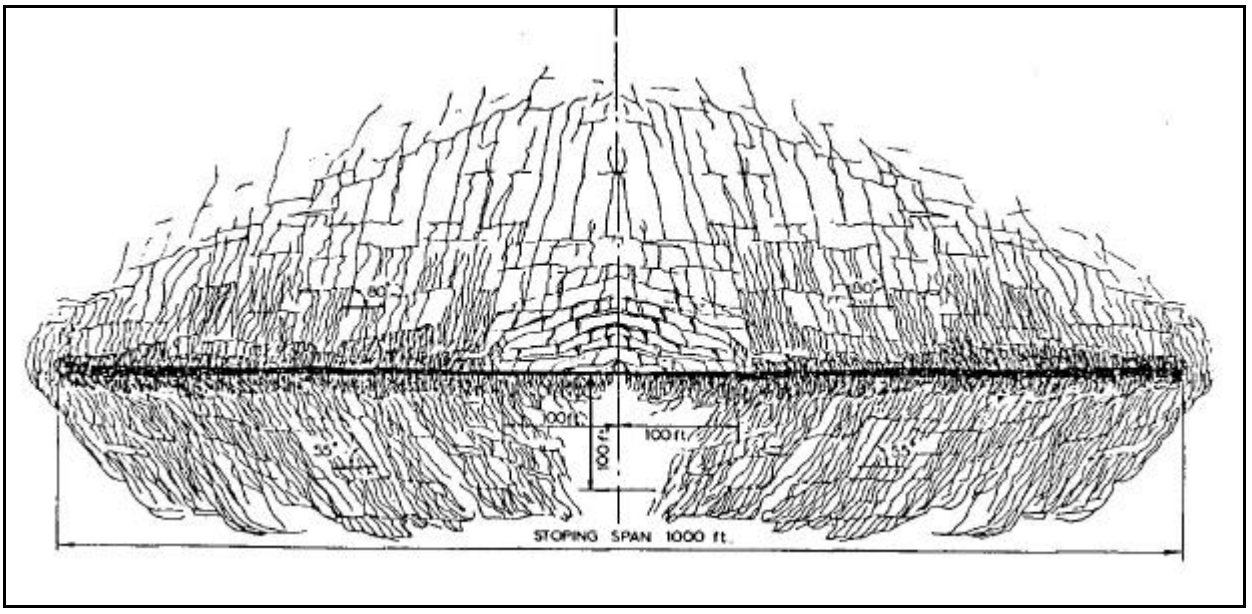

Figure 1. Proposed fracture pattern around a deep level stope (after Leeman, 1958)

Kersten (1969) made observations in a caving stope and expressed the orientations of fractures statistically. A scatter graph of orientation vs. advance is presented in Figure 2. This graph very clearly shows that (at least) two distinct fracture orientations are present. Kersten classed these fractures as type I (dipping away from the face), type III (dipping towards the face), and type II (a hybrid of type I and III). The orientations of these types relative to face advance are illustrated in the schematic in Figure 2. Observations of the fracture planes revealed that class I fractures had clean surfaces, indicating purely tensile failure. The class III fractures showed evidence of relative displacement along the surfaces, indicating shear failure.

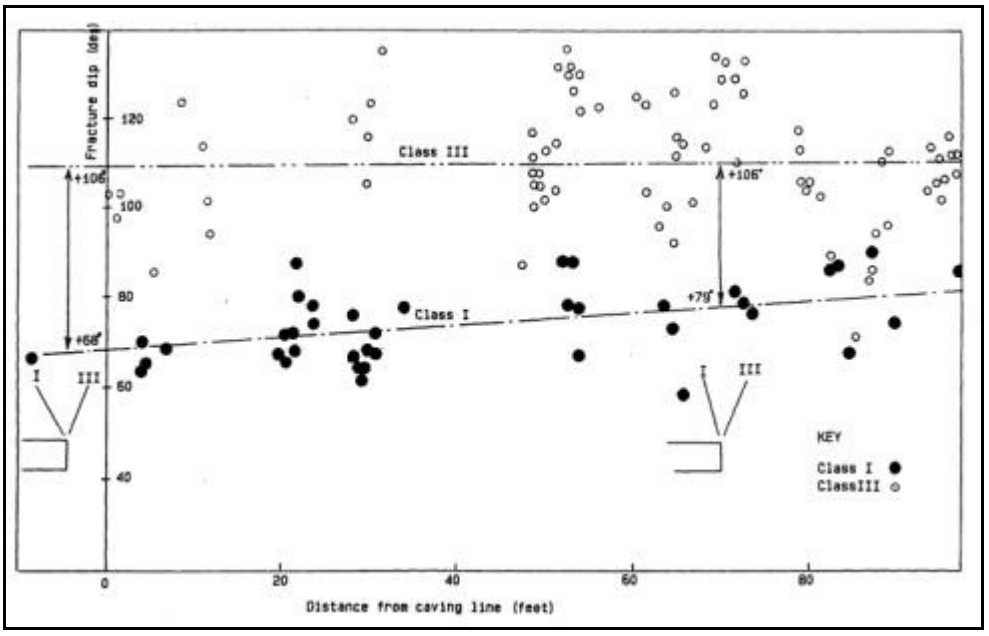

Figure 2. Distribution of fracture orientations within a caving stope (After Kersten, 1969)

McGarr (1976) observed similar groups of fractures, dipping towards the face (type 1) and dipping away from the face (type 2). A schematic is presented in Figure 3. He differentiated between the groups by observing that type 1 fractures exhibited little or no crushing, while crushing was observed on type 2 fractures. He concluded that type 2 fractures were certainly shear fractures, although he was less clear about the origions of type 1 fractures.

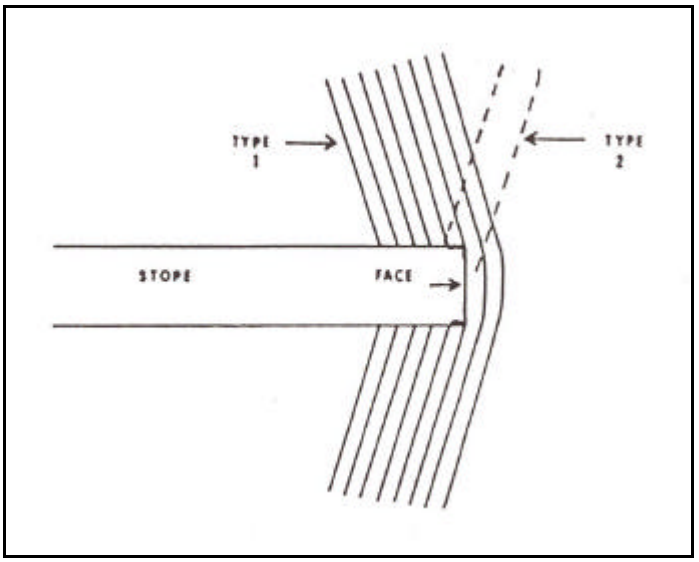

Figure 3. McGarr's (1976) fracture classification

Gay (1976) performed laboratory tests on solid rock blocks containing "excavations" representing stopes. The classification system he used designates type 1 fractures in McGarr's work as type I fractures, and type 2 fractures as type II. These fractures are illustrated in Figure 3. It was noted that type I fractures appeared first, at lower stress levels and for smaller spans. Type II fractures appeared later. The type II fractures were initiated before they became visible and exhibited shear displacement, leading to local crushing. This work showed quite conclusively than type II fractures could be legitimately termed "shear fractures".

Roering (1978, 1979) found sets of inclined fractures ahead of the face. The fractures were grouped into three types: Type I fractures parallel to the face and exhibiting no shear displacement, type II fractures sub-parallel to the face, dipping towards or away from the face, with a pronounced shear displacement, and, type III fractures similar to type I but with a very shallow dip.

Adams *et al* (1981) adopted a similar classification system, which is graphically illustrated in the stope cross-section presented in Figure 4. This investigation aimed to characterise the fractures. The following was noted for each type:

- Type I
    - The most common type of fracture.
    - Essentially vertical fractures with a strike length of 10 m or more.
    - These fractures are planar, and, notably, tend to cut through larger grains.
    - The dip of the fractures decreases with distance from the stope horizon, e.g. the fractures are nearly vertical just above and below the reef plane and dip at 55^0 at a distance of 45 m into the footwall. The density of fracturing also decreases with distance from the reef plane.
    - Though small (< 50 mm) displacement is observed along the fracture planes, this is a secondary process not associated with the formation of the fractures.

- Type II
    - Displacement is observed on the plane of the fractures (up to 140 mm).

- Fractures are inclined between 60^0 and 75^0 to the stope face, dipping away from the direction of face advance in the hangingwall, and dipping in the opposite direction in the footwall.
- The fractures are composed of broken and crushed material and may be several centimetres thick.
- The fractures may extend 7 m above and below the reef plane and may have strike lengths exceeding 70 m.
- These fractures provide a mechanism for rock ahead of the face to move horizontally into the stope, and for rock in the footwall and hangingwall to move vertically into the stope.

- Type III
  - Low angled fractures occurring in areas where type I and II fractures already exist.
  - They are secondary fractures that develop in intact rock close to the face.
  - Dip at 30^0 to 40^0 in the direction of face advance in the hangingwall and in the opposite direction in the footwall.
  - Do not extend more than 3 m into the hangingwall and have a strike length of less than 5 m.
  - Physically indistinguishable from type I fractures.

Type I and II develop some distance ahead of the face (up to 10 m), while type III fractures appear close to the face. Shale layers, spaced 0.5 m to 1 m above and below the stope horizon, tend to inhibit the propagation of fractures, with only the largest fractures propagating across these layers. Individual fractures, therefore, seldom extend for more than 3 m.

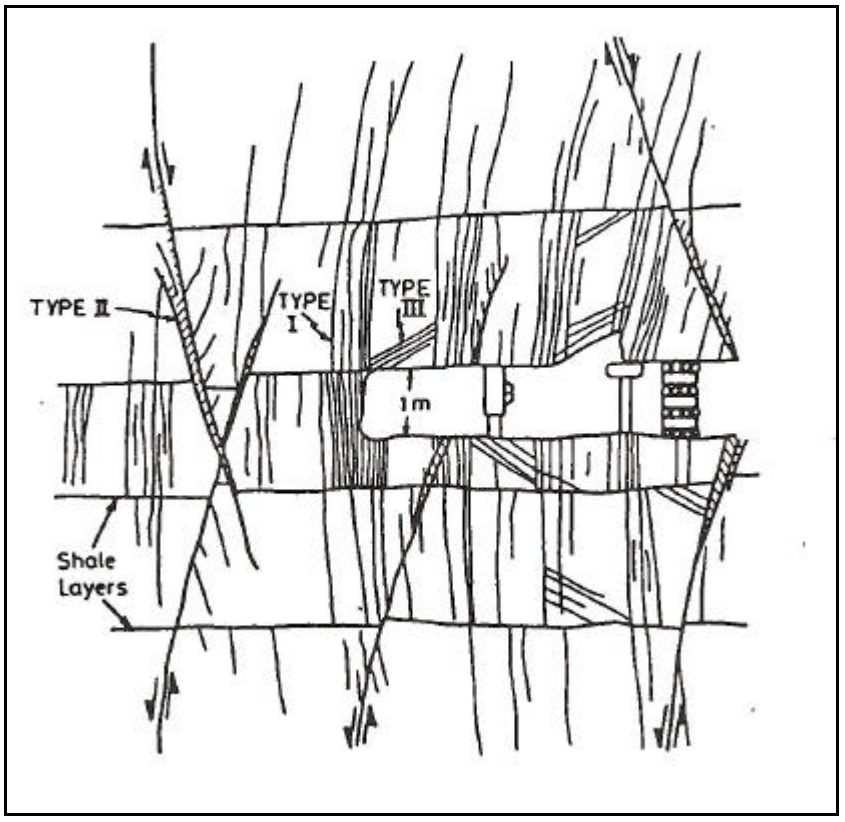

Figure 4. Fracture classification after Adams *et al*. (1981)

This investigation also showed that the extent of fracturing ahead of the face could be directly related to the energy release rate (ERR - effectively, rate of mining), but the fracture density was

unaffected by ERR. It was also concluded that seismicity had little influence on the nature of the fracturing.

Brummer and Rorke (1984) pointed out that the various fracture classification systems were inconsistent, unclear and caused confusion. A mechanistic classification system was proposed. Essentially, two types of fracture are recognized. Extension fractures are effectively tensile fractures, which form parallel to the major principal stress direction. They are assumed to appear where confinement is low. These are analogous to type I (and type III in Adams, *et al.*) fractures in the preceding works. Shear fractures, similar to type II fractures, are also recognised. These fractures are composed of multiple closely spaced extension fractures and characteristically exhibit relative shear displacement along the fracture plane. They are associated with regions of high confinement.

Brummer and Rorke's (1984) work concentrated on exposure of large sections of the hangingwall in various mines. Photographic techniques were used to map these exposures. Fractures were subsequently classed according to the degree of comminution observed on the fracture surfaces (indicating shear or extension fracturing). An example from an experimental site at Doornfontein Gold Mine is presented in Figure 5. Thick lines indicate shear fractures, thin lines indicate extension fractures, and dotted lines show geological features, e.g. parting planes.

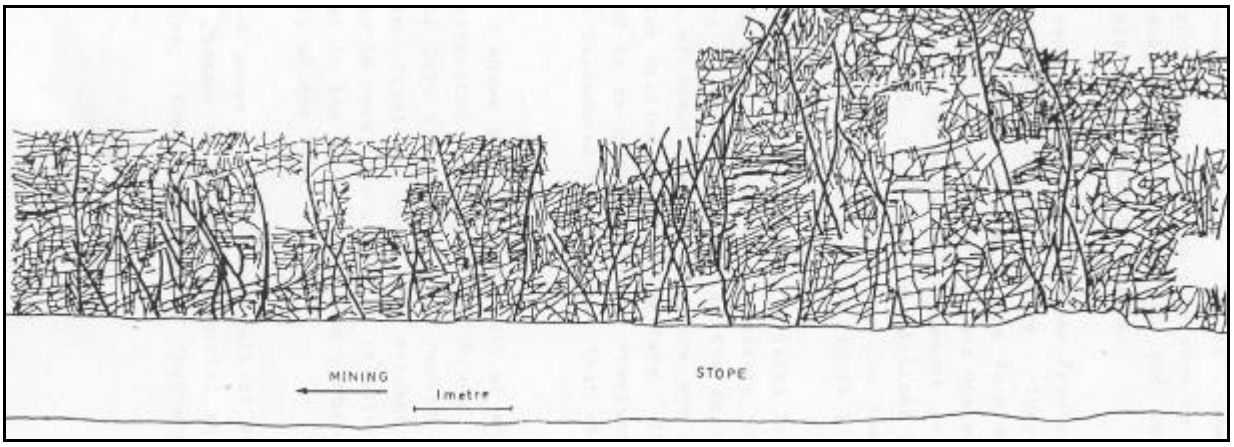

Figure 5. Hangingwall exposure from Doornfontein Gold Mine (after Brummer and Rorke, 1984)

From observations at these sites, a schematic was proposed (Figure 6), representing chronology and location of fracture formation around tabular stopes.

- Zone 1
  - This is where stresses are highest and where the first excavation-induced fractures will appear.
  - Microfracturing in tension builds macroscopic shear fractures, which dilate towards the stope.
  - Spacing of these fractures is fairly regular

- Zone 2
  - The fracturing is this zone is best described in the authors' own words:
    - "On a macroscopic scale, movement is observed on the shear planes formed in Zone 1, which breaks the rock into more or less wedge-shaped interlocking pieces, of the order of 1 m in size."
    - "On an intrablock scale, local high stresses at asperities and other point contacts cause individual blocks to split in a direction more or less parallel to the maximum principal stress direction, thus generating a number of extension or tensile fractures, with little or no relative displacement. As the face advances, however, shear movement along some of these

fractures is possible. For reasons which are not yet fully understood, this process occasionally does not occur, resulting in a “hard patch” of unfractured rock on the face.”

- Zone 3
  - Longitudinal splitting occurs in the direction of major principal stress – extension fracturing.

- Zone 4
  - Describes the zone between the hangingwall surface and the first parting plane above the stope
  - “…relatively passive, fractured layer of rock”.

- Zone 5
  - Similar to 4, only in the footwall.

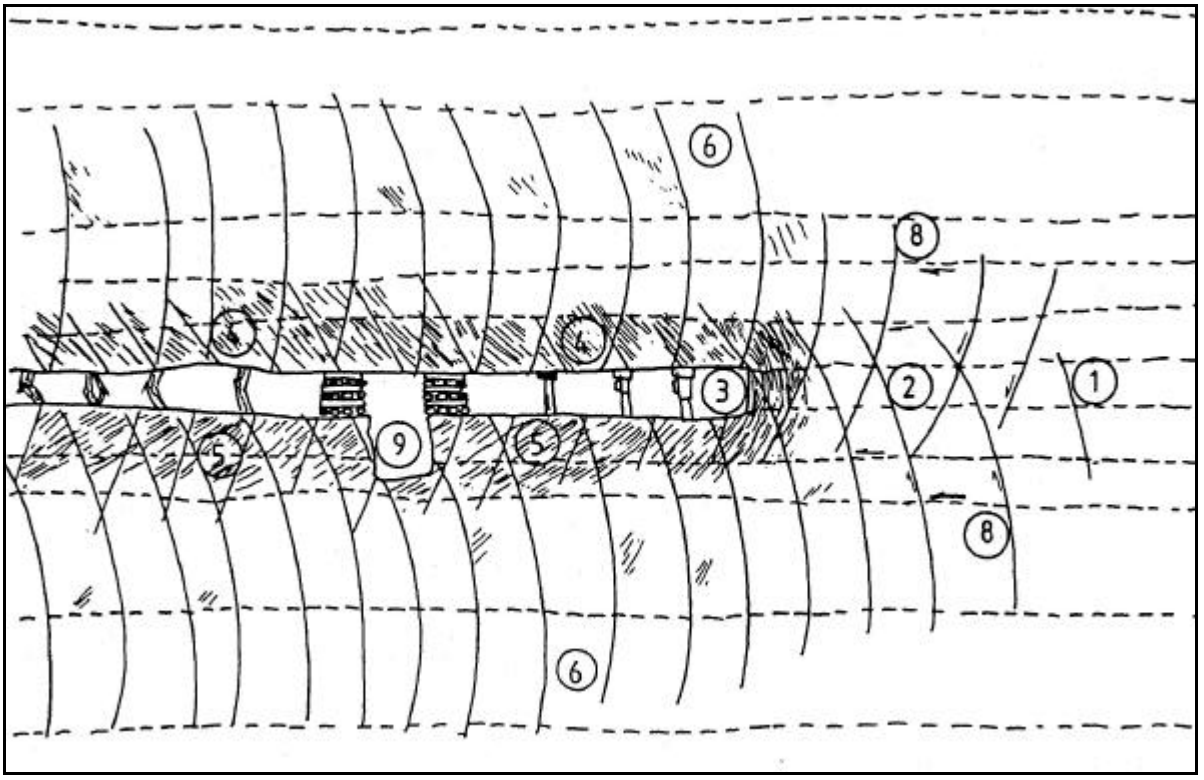

Figure 6. Schematic of fracture distribution (after Brummer and Rorke, 1984)

This schematic is similar to that presented by Adams, *et al.* but emphasises that extension fractures (type I) are not necessarily vertical, and tend to dip away from the face.

Brummer (1987) presented a thorough literature survey on the subject of stope fracturing and pointed out that previous researchers had observed periodicity in the fracture pattern. Adams and Jager (1980) had suggested that periodicity was due to the appearance of zones of extension fractures. Crucially, it was also noted that this phenomenon was not associated with the drill-and-blast cycle, as it had been observed in mechanically excavated stopes.

Jager and Ryder (1999) presented the most recent work on hangingwall geometry and condition for deep level mining. The classification is similar to that of Adams, separating the fracture types into shear and extension fractures. Shear fractures in this work are assumed to appear first, followed by “primary” extension fractures. Both form at the edge of the fracture envelope.

"Secondary" extension fracturing occurs very close to the face, oriented vertically at the face, and curling around and dipping at up to 70^0 in the hangingwall.

Low-inclination fractures were also identified, dipping in at between 20^0 to 40^0 towards the face. These were not mentioned by Brummer, but were considered by Adams, *et al*. They are, however, associated with the "hard patch" of unfractured rock noted by Adams. Termination of these fractures against steep-dipping fractures leads to the assumption that these are younger fractures.

Fractures parallel to the stope hangingwall (and hence the direction of stratification) were noted and classified as young fractures by the same logic as above. These fractures appear behind the face and are associated with an increase in horizontal stress (and relaxation of the high horizontal stress). It has also been suggested that they may form as a result of repeated dynamic loading.

Local conditions may greatly influence the fracture pattern around a stope. For example, the VCR hangingwall is generally one of two types of lava, with the footwall consisting of a variety of materials. The influence of these various conditions on fracture pattern is illustrated in Figure 7.

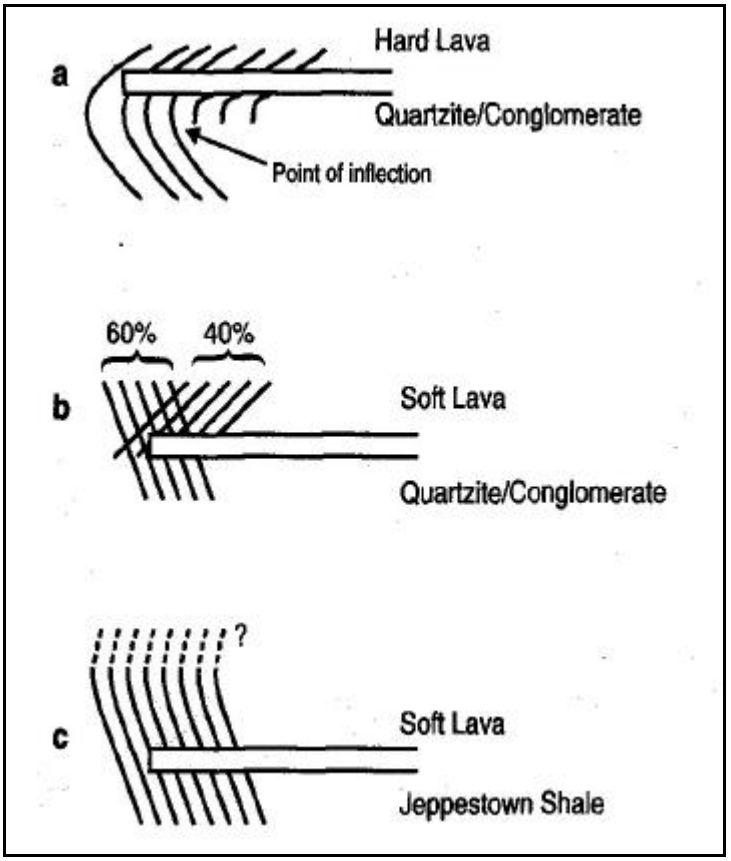

Figure 7. Variability of fracture pattern in the VCR due to hangingwall and footwall material

Daehnke *et al*. (2000) followed the convention of Gay and Jager (1986), identifying four types of extension fracture (types 1 through 4) and one type of shear fracture (type 5). The characteristics of these types of fractures are presented in Table 1.

Table 1. Characteristics of various types of mining-induced fractures (After Daehnke, *at al.* 2000)

TYPE	SPACING		PERSISTENCE (STRIKE)		PERSISTENCE (INTO HW)	DIP
	AVERAGE	RANGE	AVERAGE	RANGE	RANGE	RANGE
1	0,07	0,05 - 0,5	1,5	0,8 - 6,0	1,0 - 5,0	60^{O}-80^{O}
2	0,07	0,05 - 0.5	1,5	0,8 - 4,0	1,0 - 5,0	60^{O}-80^{O}
3	0,03	0,01 - 1,0	1,5	0,8 - 4,0	1,0	20^{O}-40^{O}
4	0,3	0,1 - 0,5	0,3	0,1 - 0,5	1,0	0^{O}-20^{O}
5	3,0	1,0 - 6,0	8	5,0 - 30,0	7,0	100^{O}-120^{O}

2.2.2. Platinum mine hangingwall conditions

Hangingwall conditions in platinum mines are very different to those encountered in gold mines, both because of the different stratigraphy and rock types, and because platinum mining typically occurs at relatively shallow depth. Very little mining-induced fracturing is observed around panels in platinum mines. Pre-existing jointing, bedding and geological features contribute towards hangingwall stability problems. The hangingwall within the platinum environment is characterised as “blocky”, consisting mostly of solid rock blocks, separated by joints, and terminated along horizontal discontinuities.

In the Merensky Reef, the first prominent parting parallel to stratification between 8 m and 30 m above the stope horizon, allowing for the formation of a thick massive beam in the hangingwall. Joint spacing is much greater than that of stress fracturing. The dominant joint sets have joint spacings typically ranging between 0.5 m and 2 m. Jointing is also not very persistent and the typical hangingwall is therefore competent and easy to support. Problems arise where domes, potholes and faults are present. Domes are potentially lethal features, resulting in many falls-of-ground, and are unfortunately very difficult to identify prior to the fall-of-ground. Shallow fractures are often present around domes – it therefore makes sense that any such fractures should be supported with rock reinforcement.

Conditions in the UG2 are invariably more challenging. The existence of three chromatite parting planes in the hangingwall (the “triplets”) results in potential hangingwall instability throughout. The first of these “triplets” can lie anywhere between a few centimetres to 3 m above the reef plane. Rockbolts are frequently used to support the UG2 hangingwall, effectively clamping the layers in the hangingwall together as in a coal mining support system (Watson, 2001).

2.2.3. Quantification and influence of horizontal stress

Large horizontal displacements into the stope from the face area indicate that significant horizontal stresses are present. These compressive forces serve to clamp steep hangingwall fractures together, effectively increasing the stability of the hangingwall. A secondary consequence of the presence of these stresses is that shearing along stope-parallel discontinuities, if present, is initiated. This causes the contacts to lose cohesion and bedding separation to occur. This contributes to vertical displacements observed in the hangingwall.

Horizontal stresses may limit or encourage slip, depending on the angle of the discontinuity and the contact properties.

Squelch (1990) attempted to quantify horizontal stresses in the hangingwall by measurements up to 2.5 m into the roof. This work was performed to evaluate the difference between horizontal stresses in backfilled and conventionally supported stopes. Stresses varying in magnitude from 1 MPa to 20 MPa were found in the conventionally supported stopes. While the major principal stress was compressive, tensile stresses were found in the minor principal stress direction. The backfilled stopes were found to be in bi-axial compression, which implies a more stable hangingwall.

2.2.4. Hangingwall deformation and failure

Jager and Ryder (1999) presented a schematic of deformation around a typical deep-level stope. This model is presented in Figure 8.

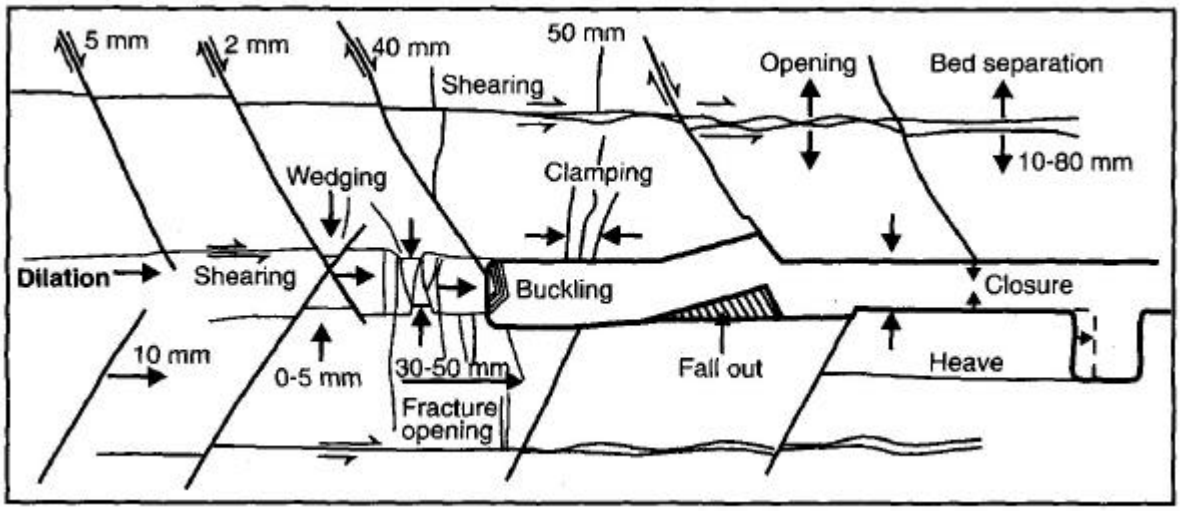

Figure 8. Deformation around deep-level stopes (after Jager and Ryder, 1999)

It has been shown that dilation of the face into the excavation can be as much as 60 mm per metre of face advance. Horizontal movements were also found to be present in the footwall and hangingwall. These are largely resisted by the rock and result in the confining stresses so crucial to hangingwall stability. This horizontal compression also results in shearing along stope-parallel bedding planes as mentioned above.

Daehnke *at al.*(2000) suggested the following mechanisms of hangingwall beam failure based on numerical models and on underground observations.

- cantilever failure of hangingwall beam;
- deadweight failure of hangingwall beam;
- shear failure at the abutment; and
- buckling failure of hangingwall beam due to high horizontal stresses.

According to Daehnke *at al.*, the abutment shear failure involves unrestrained slip and vertical movement of the block at the edge of the hangingwall beam. Slip in this area is caused by large shear stresses that are typically seen at the edges of excavations. It is essentially a local failure, but fallout of this block may reduce horizontal confinement to the extent that the entire beam falls out. Cantilever failure is similar, but comes as a result of rotation of the block at the edge of the beam, which reduces the contact area and hence leads to fallout. The main difference

between these two failure mechanisms is that the shear failure is independent of the beam span, while cantilever failure is solely attributable to an excessive unsupported span.

It was noted that a combination of these mechanisms can occur simultaneously. These mechanisms are related to the expected resultant loading on bolts installed within such hangingwalls.

2.2.5. Summary of gold mining hangingwall profiles

Three basic geotechnical conditions typify most of the South African gold mine stoping environments. These are exemplified by the conditions in the Carbon Leader, VCR (Ventersdorp Contact Reef) and Vaal reefs. Each of these has a characteristic hangingwall profile, from the spacing of stratigraphic layers to the orientation and frequency of mining-induced fractures. These generic hangingwall types have been identified and outlined by Jager, (2001) and Roberts (2001), and are presented below.

2.2.5.1. Vaal Reefs generic hangingwall

The Vaal Reefs, although occurring in the Krugersdorp formation is similar to several of the Kimberley reefs in that they have well bedded hangingwall strata providing many parting planes. The generic pattern is illustrated in Figure 9. The stoping width is typically between 1 m and 1.6 m, with the hangingwall consisting of medium strength argillaceous quartzite. The dip is less than 15^0. Closure rates are of the order of 20 mm/day in a two-day cycle. Bedding and fracturing conforms to the following patterns:

- Shear fractures:
  - 3 m spacing
  - 60^0 to 80^0 orientation dipping towards the face
- Extension fractures:
  - 0.2 m spacing
  - $70^0 – 80^0$ orientation dipping away from the face
- Bedding
  - 0.3 m spacing
  - sliding is observed on the bedding planes

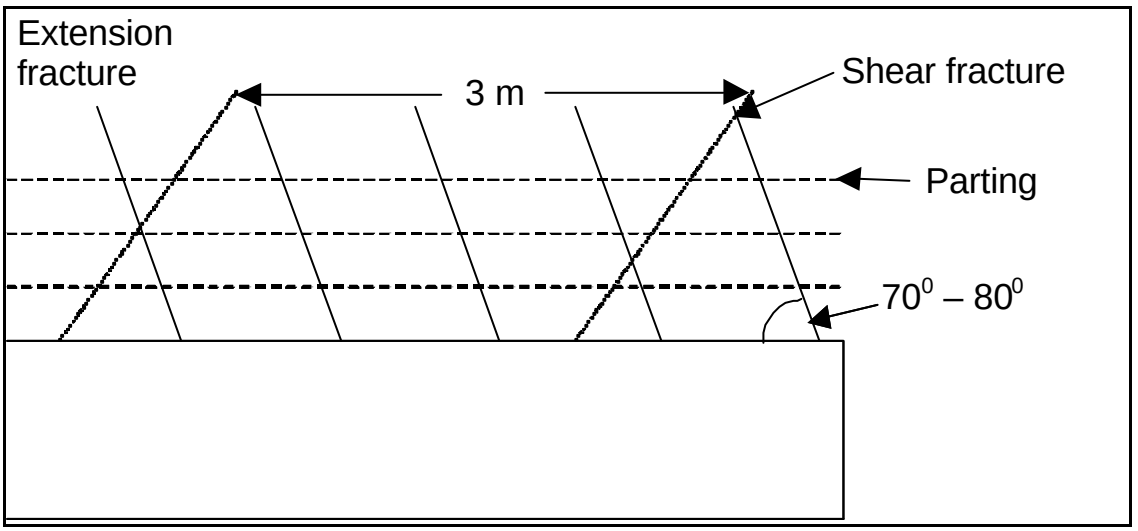

Figure 9. Generic Vaal Reefs hangingwall

2.2.5.2. Carbon Leader generic hangingwall

The Carbon Leader reef is typical of Basal, Main, Elsberg, Bird and Doornkop reefs. The stoping width is typically around 0.9 m to 1.3 m, but occasionally up to 4 m. The rock mass is particularly strong in this region, often exceeding strengths of 300 MPa. There are few bedding planes, if any in this region, except for those around the Green Bar layer which is encountered 1.8 m to 2 m above the stope. Fracturing is intense and complex, with discontinuity spacings of 0.01 m in some places. Low-angle fractures are also commonly encountered. Dip is typically 20^0. The closure rate is around 10 mm/day in backfilled stopes, and up to 50 mm/day where backfill is absent.

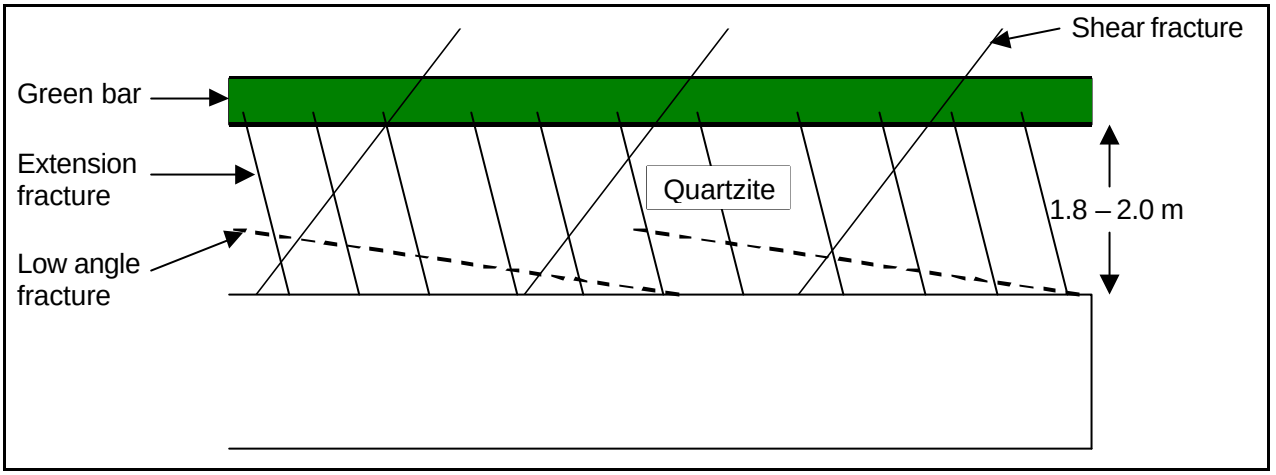

Figure 10. Generic Carbon Leader hangingwall

2.2.5.3. VCR generic hangingwall

A typical VCR stope is illustrated in Figure 10. Hangingwall behaviour is dominated by a combination of fracturing and jointing. The presence of low-angle jointing and near-vertical extension fracturing results in a blocky hangingwall. Quartzite is sometimes present in the immediate hangingwall, resulting in a skin of highly fractured (0.05 m spacing) material between the reef and the lava. The hangingwall is most often high-strength hard lava (200 – 400 MPa), while the composition of the footwall is variable (see Figure 7). The deformation characteristics of the hangingwall are such that a large elastic response is observed after blasting. The overall closure rate is in the order of 10 mm/day. The stoping width is highly variable: from 1 m to 10 m.

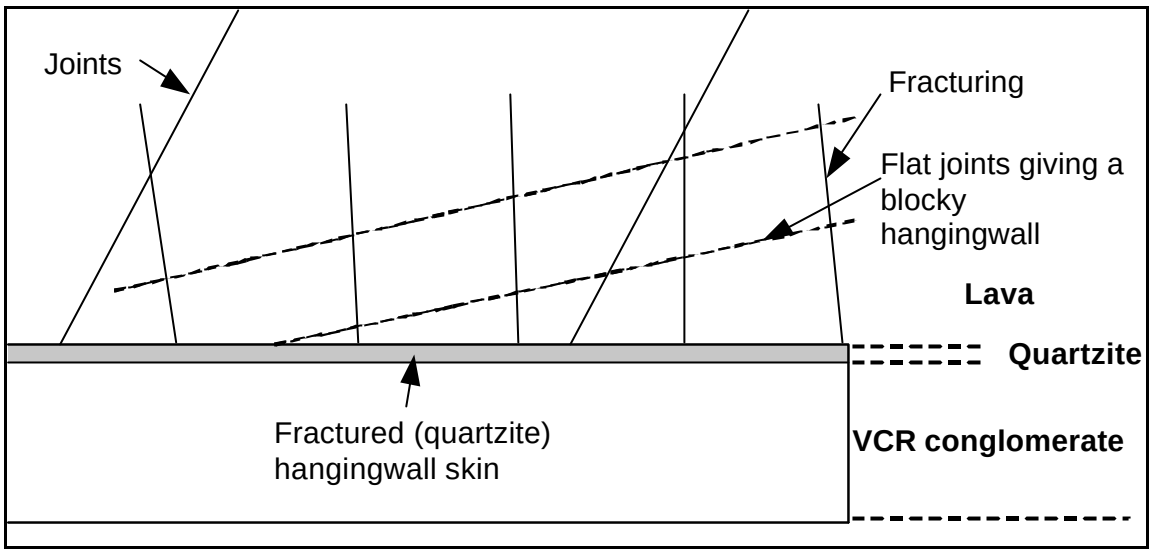

Figure 11. Generic VCR hangingwall

2.3. Description of rockbolts and rock reinforcing elements

Rockbolts refer to any form of reinforcement in the form of a bar, cable or tube inserted into boreholes in the rock mass, and anchored by grouting, friction or mechanical means.

Potential instability within the fragmented rock surrounding an excavation may be realised through relative displacements between intact rock blocks. Ultimately, potentially unstable blocks are rotated or moved such that adjacent blocks no longer supply enough confinement to prevent these blocks from falling out. In this situation, the function of rock reinforcement is to reduce these relative displacements and hence reduce the probability of blocks falling out. This is the basic principle of rock reinforcement. Mechanistically, it is possible that an arching effect is created by holding adjacent blocks together, which can provide additional confinement to adjacent portions of the hangingwall. In this way, the reinforcement assists the rock mass to support itself.

In specific applications, rock bolting may be used to suspend the fragmented zone by tying the entire tendon back to relatively stable ground deeper into the rock mass. Cable bolts are typically employed in this application. This method aims to apply a compressive force on the portion of the rock mass lying between the surface of the excavation and the end of the bolt through mobilising tensile forces in the bolt. This application is often termed “suspension”.

Another application of rockbolts is beam building. This strategy is typically employed in the coal mining industry, where the excavation is overlaid by seam-parallel parting planes. By clamping these strata together, a stack of thin beams is converted to a single beam with an effective thickness equal to the rockbolt length. This approach is even more effective when combined with the suspension principle mentioned above. Rockbolts employed in this scheme are invariably pre-tensioned to reduce immediate bed separation (owing to the delay between excavation and bolt installation), and to ensure that the full response of the reinforcing is mobilised when additional stresses are imposed (Van der Merwe, 1998).

This investigation concentrates on the reinforcement aspect of rock bolting. Short bolts are much easier to install than longer bolts, and often practical considerations only allow enough time for short bolts to be installed over a single production cycle within a working stope. Such bolts may not be long enough to penetrate stope-parallel bedding planes and hence function in the beam-building or suspension roles. This limitation determines which bolt type is most appropriate. In the reinforcing role, it is important to bond with the rock along as much of the bolt

length as possible. Pre-tensioning of bolts is unnecessary. Full-column grouted bars or friction anchors (Split Sets or Swellex) are therefore most appropriate for this application.

Rockbolts and reinforcing elements are classified here according to the mechanisms by which they operate. The following types of reinforcement were identified by Thompson and Windsor (1992):

- continuous mechanically coupled tendons (CMC) – fully grouted bars and cables;
- continuous frictionally coupled (CFC) – Split Sets and Swellex bolts; and
- discrete mechanically and frictionally coupled (DMFC) – Mechanical or resin end-anchored bars and cables.

2.3.1. Continuous mechanically coupled (CMC) rockbolts

As identified by Thompson and Windsor (1992), these types of reinforcing elements rely on a securing agent, typically cement grout or resin, which fills the annulus between the element and the borehole wall. Loads are transferred from the rock mass to the tendon via the grout along the entire length of the tendon. Reinforcing elements used in conjunction with grouts often have variable cross sectional shapes along the length so that a geometric interference is created, thus increasing the strength of the grout-tendon bond.

They can be described as passive but stiff support units requiring deformation of the rock to generate support forces. The most widely used type in South African mines is the Shepherd's Crook (a smooth bar or rebar bent into a crook-shape) and is mostly used in tunnels. Figure 12 shows a load-deformation curve of a resin-grouted rebar loaded in tension across a joint.

Certain types of CMCs can be pre-tensioned. Typically this would be a resin bolt where a fast setting resin capsule would be inserted first to end-anchor the bolt followed by slow-setting resin capsules until the hole is full. The bolt can be pre-tensioned before the slow-setting resin hardens. Depending on the application, the reinforcement system will hence be active from installation, and will be stiffer when subjected to load (Stillborg, 1994). It is not known how pre-tensioning of bolts installed in a highly fragmented hangingwall would influence the stability of the rock. Shepherd's Crooks are generally not tensioned, though cable bolts in the South African environment, very often are. They have little yield capacity, as strain in the tendon will be concentrated in the area providing the deformation (i.e. a dilating fracture).

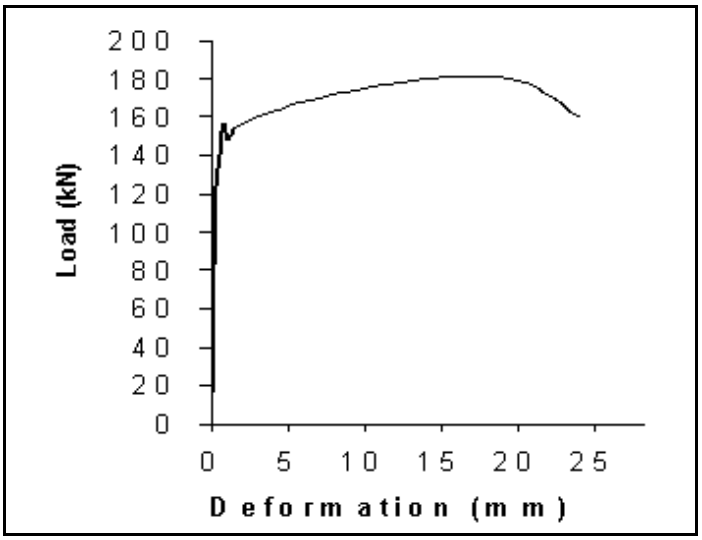

Figure 12. Resin grouted rebar – tensile loading across a joint (after Stillborg, 1994).

2.3.2. Continuous friction coupled (CFC) tendons

With these types of tendons, the reinforcing element is placed in direct contact with the rock. This means that CFCs are coupled by a frictional interface between the rock and the tendon itself. They have a radial pre-stress, which provides a force normal to the friction interface. The most commonly used types are the Split Set and Swellex systems. The Split Set is an oversized split tube forced into an undersize hole, while the Swellex rockbolt is an undersized element expanded into an oversize hole by water pressure.

Figure 13 illustrates a typical result from a tensile loading test across a joint for a Split Set. It can be seen from the graph that the bolt starts to slide at about 50 kN after the frictional resistance is exceeded. The sliding is preceded by no measurable rockbolt deformation. The strain is distributed over a significant length of the unit and the whole unit can slide, thus providing some degree of yieldability. However, the amount of yield depends on rock conditions and borehole geometry. It should be noted that the yield range of the Split Set is limited, as applied load cannot be maintained after rockbolt deformation.

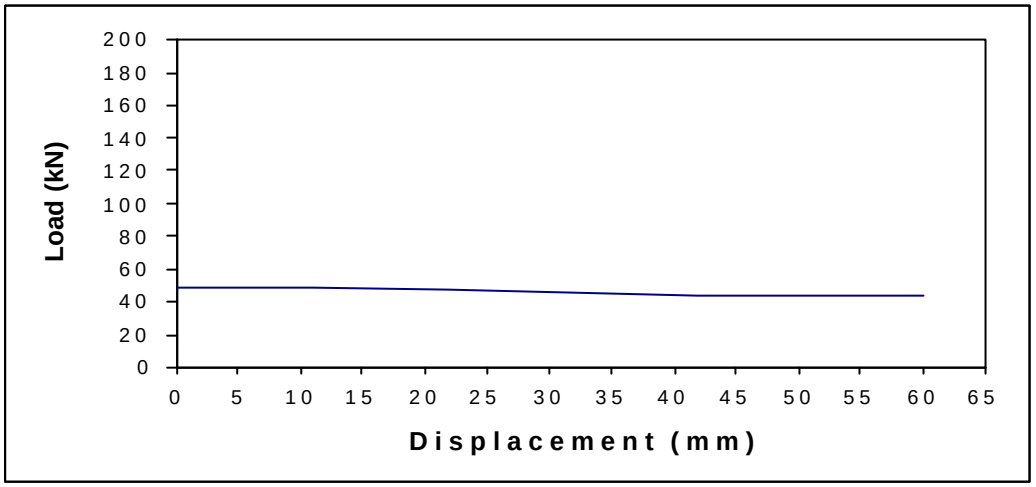

Figure 13. Split Set type SS 39 – tensile loading across a joint (after Stillborg, 1994).

2.3.3. Discrete mechanically and friction coupled (CMFC) tendons

Discrete mechanical and friction coupled tendons are coupled to the rock over a discrete length of the tendon, usually concentrated on or located at the end of the tendon within the rock mass. This coupling, which must be sufficiently strong to mobilise the full strength of the reinforcing element, is either in the form of some sort of mechanical device, e.g. an expansion shell (discrete friction coupled), or by means of grout, usually resinous, at the anchoring end (discrete mechanical coupled).

An integral part of these devices is a base plate or bearing plate, which allows load to be transferred from the rock to the tendon. Such tendons are active in that they can be tensioned upon installation. Examples of CMFC tendons are the expansion shell bolt, end anchored cable bolt, resinous plain bar, deformed bar, etc. Strain generated in the tendon by dilation of the rock mass can be distributed over the full length of the tendon, thus providing some small degree of yieldability.

A load-displacement curve of a typical expansion shell rockbolt is shown in Figure 14.

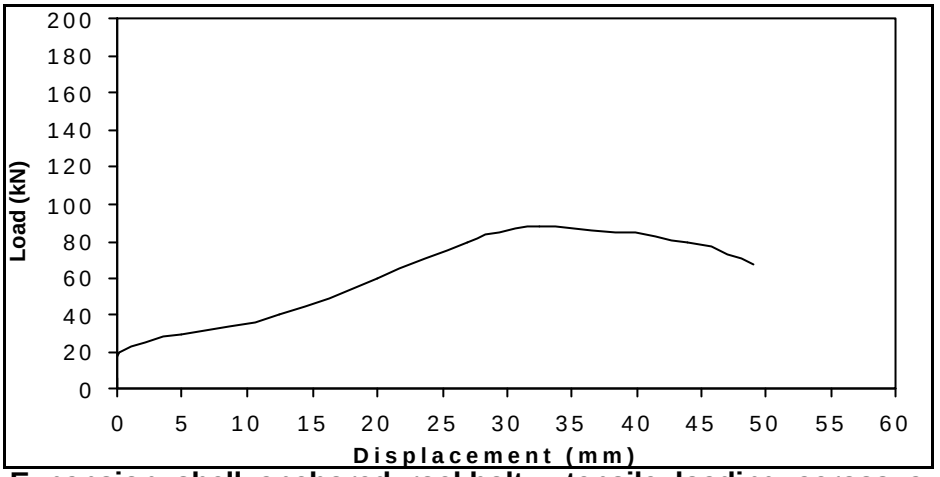

Figure 14. Expansion shell anchored rockbolt - tensile loading across a joint (after Stillborg, 1994).

2.3.4. Yielding tendons

All the above types of tendon are likely to fail under rockburst conditions if intimately connected to a sufficiently large mass of rock. As a result, yielding tendons have been developed in South Africa. The Conebolt and Durabar are two types of tendon that can yield by any practical amount, up to 500 mm, and, in so doing, absorb energy at a rate of approximately 30 – 50 kJ/m^2 for a 1 m bolt spacing. The Conebolt works on the principal of dragging the flared end of the bolt through the grouted hole, compressing the grout and generating high frictional forces. The Durabar works on the principal of deforming the steel bolt by dragging the tail of the bolt through a set of wave shapes set in the grout by the original shape of the bar. In both designs the bar is debonded from the grout.

2.4. Application of rockbolting to stope support

A review of current applications of rockbolting to stope support was undertaken in GAP606 (Daehnke *et al*. 2000). Such applications are limited in comparison to the areal support systems commonly used. Evander, Western Platinum, Vaal Reefs, Randfontein Estates and Beatrix mines use rockbolts in the stope face area at varying distances from the stope face and at different spacings. These applications are discussed below.

2.4.1. Evander Mine (Kinross)

There exists a 20-30 cm thick beam that may be up to 1 m above the reef-hangingwall quartzite contact. The beam is separated from the quartzite (UCS of 170 MPa) by a well-developed, persistent argillaceous parting. Threaded expansion shell rockbolts were used to bolt the 20-30 cm beam to the competent thick mass of quartzite above it. Rockbolts were employed on 60-65 % of all panels at Kinross Mine. Rockbolts were drilled 70° to the hangingwall over the stope face and not more than 1.3 m from the face after the blast. The choice of 70° is to accommodate both the bedding planes and the 75º faceward dipping extension fractures (see Figure 15). The length of the rockbolts used is mostly 0,9 m and occasionally 1,2 m, depending on the height of the beam above the reef-hangingwall contact.

Note that the approach here is fundamentally different from that of the current research, as the idea behind the application at Kinross is to clamp hangingwall strata together using long bolts, as opposed to using short bolts to improve stability of the hangingwall surface.

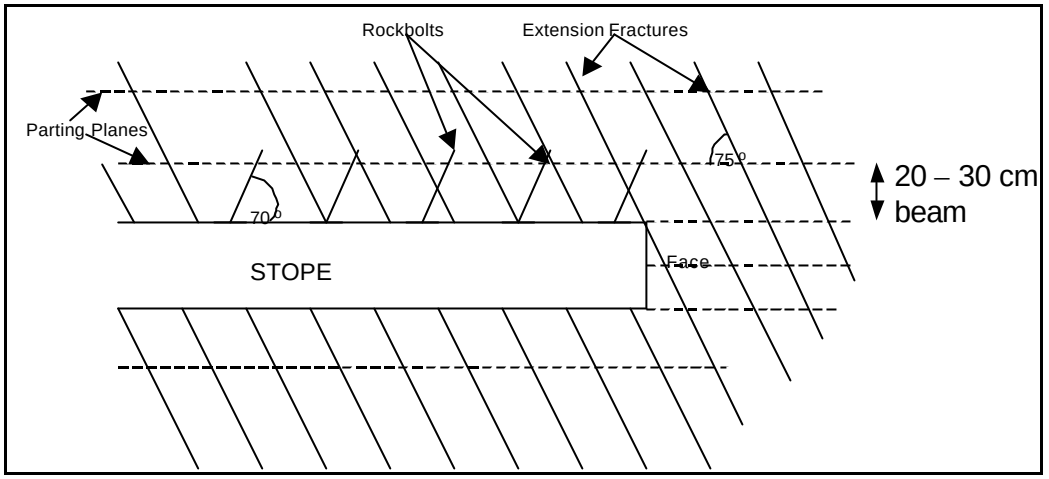

Figure 15. Inclination of rockbolts with respect to orientation of parting planes and extension fractures, Kinross Mine. (after Daehnke, *et al*. 2000)

Mine visits revealed that in some areas the rockbolting within 5 m of the face appeared to be unsuccessful, as there were many fall-outs between rockbolts. It appeared that this was due to intense cross-bedding in the area, effectively thickening the lower beam and increasing the minimum required bolt length for penetrating through the overlying beam. Bolting was, however, very successful in undercutting operations. Bolt loosening after the blast was common, though it was not clear whether this was due to poor setting of the anchor, blast-induced vibration, inadequate pre-tensioning or frittering of rock from beneath the bearing plates.

2.4.2. Western Platinum mine

As mentioned above, the UG2 reef is overlaid with thin persistent chromite layers that form weak partings in the hangingwall. The distance of these to the excavation ranges from 0.5 to 4.0 m. Rockbolts are used in the Western Platinum mine to clamp a parting 30-50 cm above the UG2 and the hangingwall pyroxenite contact. 0.9 m-long expansion shell end-anchored rockbolts are installed as close to the face as possible. Apart from some problems with incorrectly pre-tensioned bolts, rockbolting in the area appears to have been able to stabilise the strata within the stope.

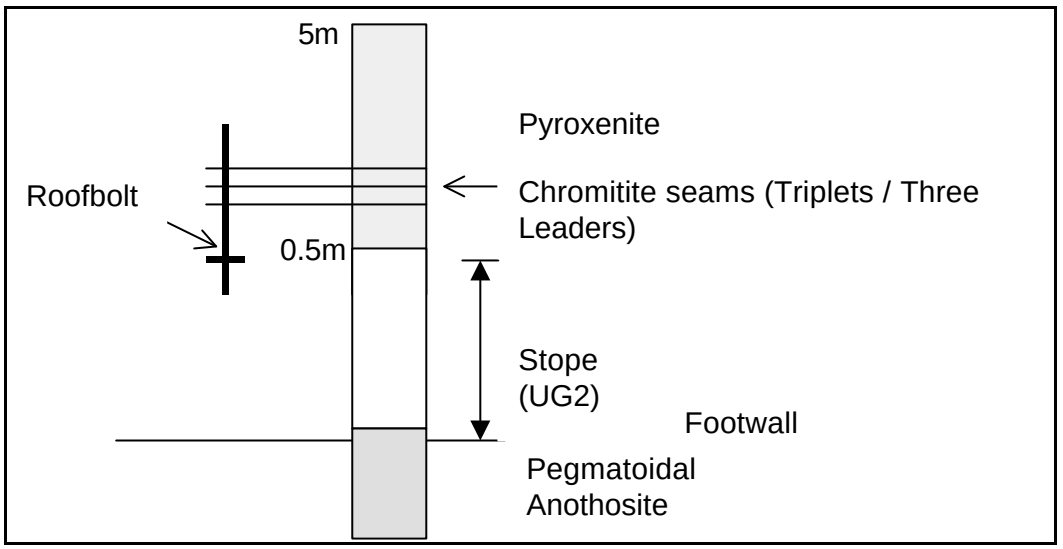

Figure 16. Application of rockbolts in the UG2 seam at Western Platinum mine (After Daehnke *et al*. 2000)

2.4.3. Vaal Reefs

At the No. 10 Shaft of the Vaal Reefs Gold Mine, rockbolting is applied to the hangingwall strata. An undulating bedding plane above the VCR prompted the use of rockbolts to tie the strata back to competent rock above. The assumed presence of a tensile zone (extending approximately 1.25 m into the hangingwall) also contributed to the decision to use rockbolts.

Expansion shell rockbolts (1,5 m long) are employed and installed at 90^0 to the dip of the strata. These bolts are full-column grouted and then manually pre-tensioned to 10 – 20 kN. Practical considerations played a significant role in the implementation of rockbolting: for example, current drill rig design could only allow rockbolting in stopes wider than1.8 m, severely limiting the application of this support methodology. Bolts are installed at least 3 m away from the face, as the grout would not have set at the time of blasting. This limited useful application of the methodology in the critical region adjacent to the face.

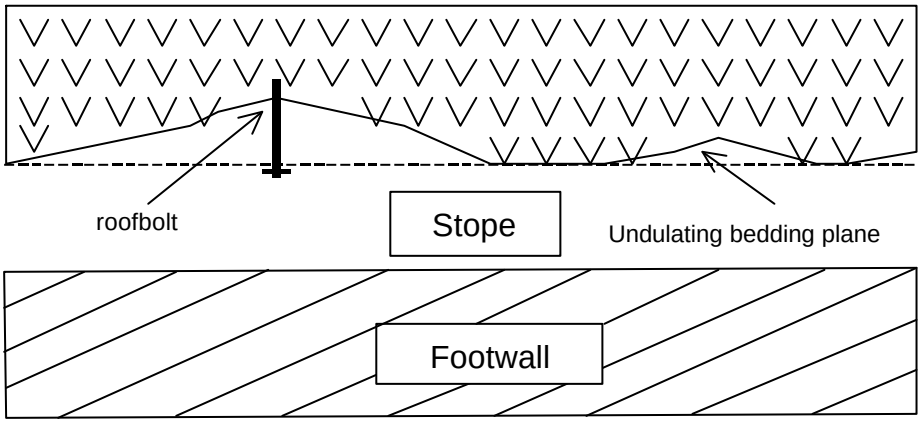

Figure 17. Roofbolting of the undulating bedding fault on the VCR Klerksdorp. (after Daehnke *et al*. 2000)

2.4.4. Randfontein Estates

The presence of a hangingwall parting at a depth of 50-60 cm above the upper Elsburg reef-hangingwall contact at some sections of No. 3 Shaft of Randfontein Estates Gold mine has necessitated the use of expansion shell rockbolts.

2.4.5. Amandelbult Mine

At the Amandelbult section of Rustenburg Platinum Mines, 0,9 m full column grouted expansion shell rockbolts are used to cater for the laminated hangingwall strata, comprising Chromite leaders within the first 30 cm of the immediate hangingwall.

2.4.6. Other in-stope applications of rockbolts

Rockbolts have been used under special conditions at West Driefontein and Kloof Gold Mines with some success.

Four-metre-long full-column grouted pre-stressed long anchors, together with 2,0 m Shepherd's Crooks, are employed to support wide reef panels in the VCR and Main Reef stopes at No. 7 Shaft of West Driefontein Gold Mine. They are installed as close as possible to the face and later serve as the permanent support. The grout used is quick setting and sets before blasting commences. The hangingwall is layered and competent.

At No. 3 Shaft of Kloof Gold Mine, hollow cylindrical steel tendons were used successfully at a depth of 2 700 m to support a 20 m panel of a 1,3 m stoping width. The tendons have coupling mechanisms and can be coupled to any length. The tendons were used as the drill steels and left in the hole after drilling was completed. Quick-setting resin was then injected through the steel tube into the surrounding rock mass and in the process the beam of hangingwall around the borehole was strengthened. The hangingwall comprises soft tuffaceous lava. This was the only method of strata stabilisation and was very successful (Geyser, 1999).

3. Laboratory testing

The aim of the laboratory testing was to determine whether the presence of short rockbolts improves hangingwall stability. Therefore, this is primarily a comparative study. The aim is to construct and test a physical model simulating a typical gold-mining hangingwall. This model had to be small enough to fit in existing testing apparatus: hence there was a need for scaling. A manageable size for the model was a 1/10th scale; this requires an unsupported span of 40 cm.

The hangingwall is treated as a discontinuous beam, supported at either end. Confining stresses are applied and vertical loads are applied to determine the strength, stiffness and energy-absorbing capacity of the beam. The results for unbolted and bolted models are examined in terms of the load-displacement relationship, and also with the aid of photographs.

The laboratory modelling described here concentrates on the second set of tests. A different set of tests was conducted prior to these, which were ultimately unsuccessful for various reasons. The first set of tests is described in the appendix.

The justification and procedure for the scaling process is described in detail below.

3.1. Analytical scaling

The scaling of one parameter affects all quantities in the model. In this case, the dimensions of the model are scaled, and the criterion for successful scaling is that the resultant deformations are scaled by the same factor. This scale factor is designated *x*, and relates dimensions and deformations as follows:

$$d_f = x\, d_s$$

where $ä_f$ is the full-size deformation and $ä_s$ is the scale model deformation. The subscripts *f* and *s* will henceforth be used to refer to full-size and scale model quantities respectively. A scale factor (*x*) of 10 is chosen for the current research.

Where dimensions are scaled, it would be expected that the associated derivatives (velocity and acceleration) would scale accordingly. However, the driving factor in the models under discussion is gravity, which cannot be scaled for obvious reasons. It is therefore necessary to scale time as well as dimensions. A simple dimensional analysis follows. Note that quantities in braces (eg. [m]) are dimensions. [m] is “length” and [s] is “time”.

$$g_f = g_s$$

$$\frac{[m]_f}{[s]_f^2} = \frac{[m]_s}{[s]_s^2}$$

$$[m]_f = x[m]_s$$

$$\frac{x[m]_s}{[s]_f^2} = \frac{[m]_s}{[s]_s^2}$$

$$[s]_f = \sqrt{x}[s]_s$$

Time is therefore scaled by the square root of *x*, the scale factor. Velocities will be scaled by the same factor as length.

Mass also needs to be scaled, which will complete the scaling procedure and indicate the scaling of all parameters, including force, energy and stress. Determination of mass scaling will also establish the required material properties for the scale model. The most important material parameters in this investigation are the stiffness (Young's modulus) and density of the material. These parameters influence the elastic response of the structure, the forces generated as a result of gravity, and the dynamic characteristics of the model. At this point, choices need to made as to the relative values of stiffness and density, as the determination of the mass scaling factor is not governed by a fixed parameter (gravity), as the time scaling factor was.

For example, if the material density is not changed between models, then the mass scaling factor can be determined by comparing masses in terms of density and volume. This results in a volumetric scaling of mass, i.e. mass is scaled down by the cube of *x*.

$$m_f = \rho_f V_f \qquad m_s = \rho_s V_s$$

$$V_f = x^3 V_s$$

$$\rho_f = \rho_s$$

$$m_f = x^3 m_s$$

Other quantities, including stress and force, can now be scaled accordingly:

$$F_f = x^3 F_s$$

$$\sigma_f = x\,\sigma_s$$

$$E_f = x\,E_s$$

Where *F* is force, *ó* is stress and *E* is the Young's modulus, subscripted for the full-size (*f*) and scale models (*s*).

The material for the scale model must therefore have a density equal to that of the full-size model, and a Young's modulus *x* times lower than the full-size model. A low stiffness concrete would therefore be ideal for the purpose of the scale tests.

3.2. Model and apparatus description

The model is intended to represent the unsupported hangingwall region between the face and the first row of permanent support. The hangingwall may therefore be treated as a discontinuous beam, supported at either end. The model itself is made up of concrete blocks, the construction of which is discussed below. The testing apparatus was designed to contain the model, supply support at either end, and to allow for application of horizontal confinement and vertical displacement loads.

The design and construction processes for model and apparatus are described in detail below.

3.2.1. Apparatus design

A conceptual diagram of the testing apparatus is illustrated in Figure 18. The apparatus must allow for application of horizontal confinement while supplying resistance to these loads. Supports with resistance to vertical loads must also be present.

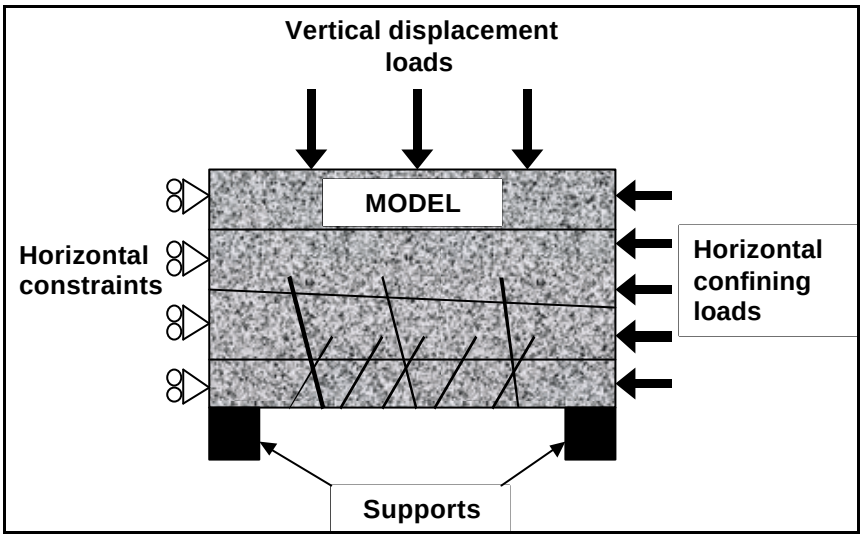

Figure 18. Conceptual depiction of the testing apparatus

The simplest means of achieving these requirements is to construct a solid box. An inflatable or expandable loading device (for example, a flat-jack) is inserted between the model and the interior of the box. Ledges representing the face and the permanent support are included in the design. An opening must be made in the upper plate of the box to allow passage of a loading piston. The piston in this analysis will be that of the Terratek machine. A section through the apparatus is presented in Figure 19.

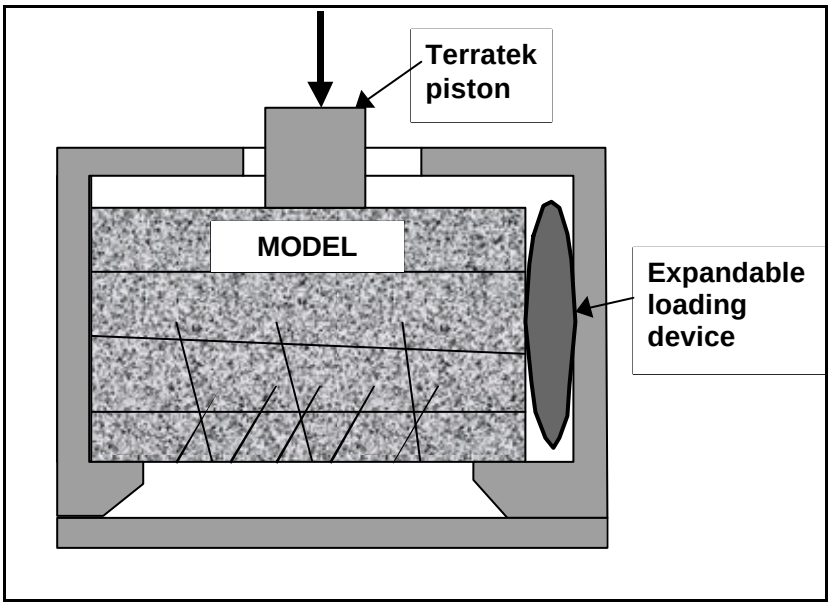

Figure 19. Section through proposed apparatus and model

A Vetter Bag, normally used for industrial lifting applications, was identified as appropriate for the task. It is an inflatable Kevlar Bag with a maximum capacity of 800 kPa.

3.2.2. Model construction

The model is essentially a series of interlocking concrete blocks. There is no in-plane variation in the geometry of the model. The blocks therefore have a constant cross-section over the width of the model. The width selected was 220 mm. The geometry for the block pattern was a single set of discontinuities representing extension fracturing. Two layers 5 cm thick are modelled. The discontinuities are spaced at 5 cm and are oriented at 80^0. The model geometry is illustrated in Figure 20. A pyramid of bricks is constructed above these two layers to ensure that the load is spread over the central 80^0 of the model.

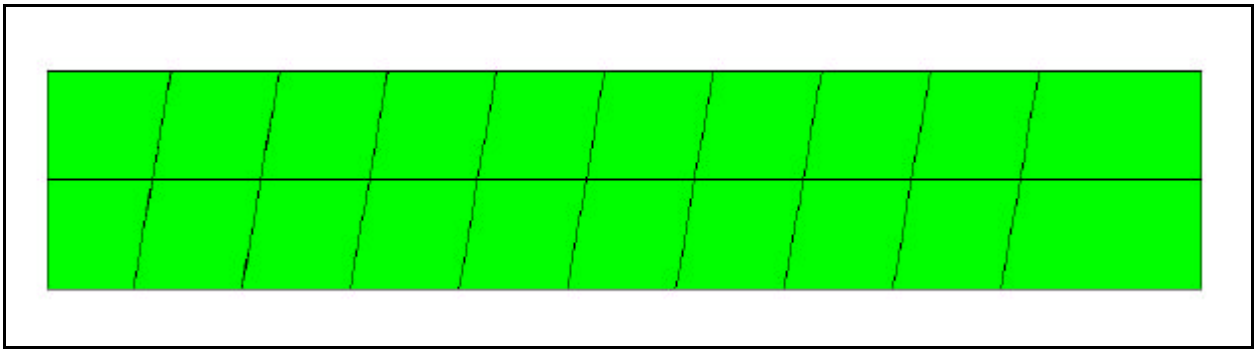

Figure 20. Conceptual diagram of laboratory model

Each layer was cast separately. Wooden trays were constructed for the casting of each layer. The extension fractures were created by suspending 1 mm-thick steel sheets across the width of the trays. Slots were cut into sides of the boxes to fix the sheets in place. Hydraulic oil was applied to all interior surfaces to facilitate disassembly and removal of the plates from the concrete blocks. The trays were placed on level ground and concrete was poured up to the 5 cm mark.

The lower layer of the bolted model was constructed slightly differently. Holes were drilled into the steel plates and 4 mm diameter nails were inserted through these plates. The nails were oriented at the correct angle and tapped into the base of the tray. Figure 21 and Figure 22 illustrate the trays for both layers before and after the concrete was poured.

The bolt-holes were spaced 10 cm apart with 5 cm free on either side, effectively modelling a 1 m in-plane spacing of bolts with symmetry. The bolts were oriented at 50^0 to the horizontal and penetrated the adjacent discontinuity at approximately the centre-height line.

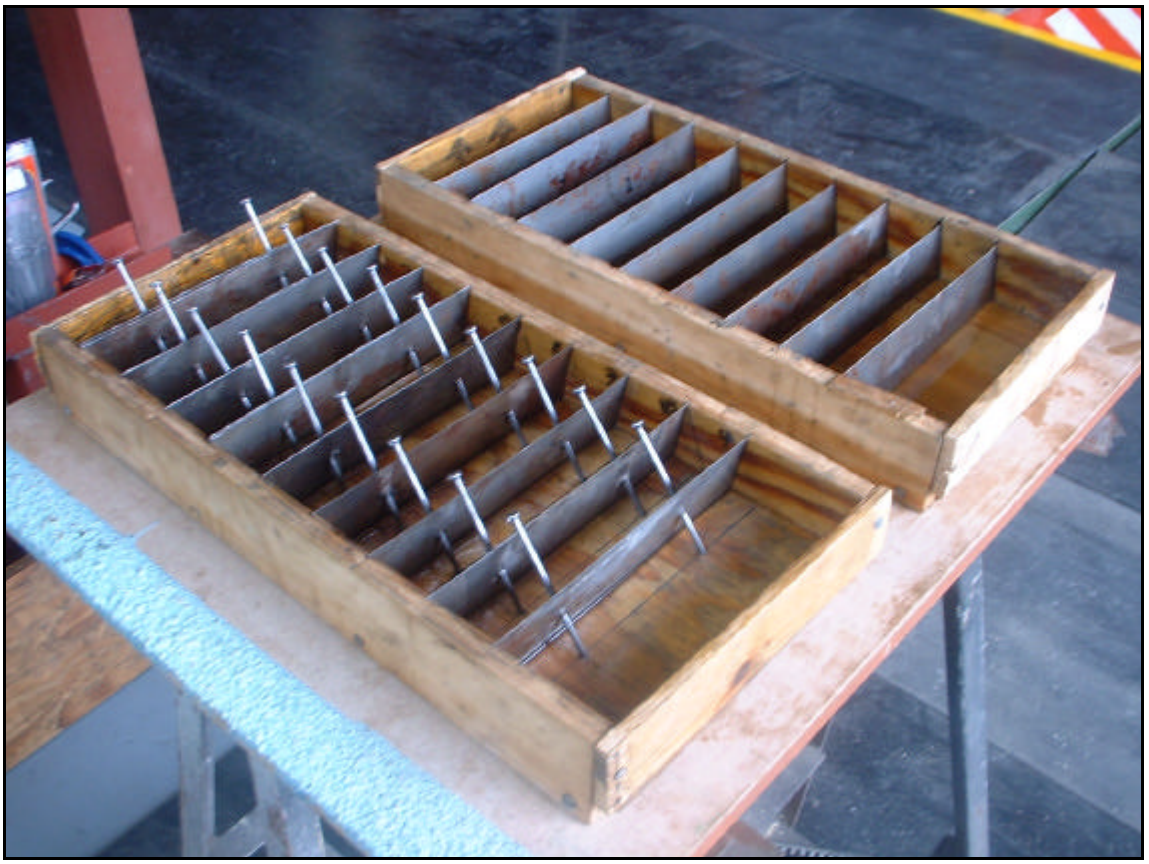

Figure 21. Tray moulds for unbolted and bolted layers prior to concrete pouring

Figure 22. Tray moulds for unbolted and bolted layers after concrete pouring

A special concrete mix was obtained from FOSROC Stratabolt. Starting with Conbextra AU, the aggregate size was reduced and high-aluminous components added to greatly reduce curing time. The concrete was permitted to cure over a period of approximately 72 hours.

Removal of the concrete blocks proved to be a simple operation. The surfaces exposed to air were quite rough in some cases and were sanded down to ensure a good fit between the blocks. The final assembled model is illustrated in Figure 23.

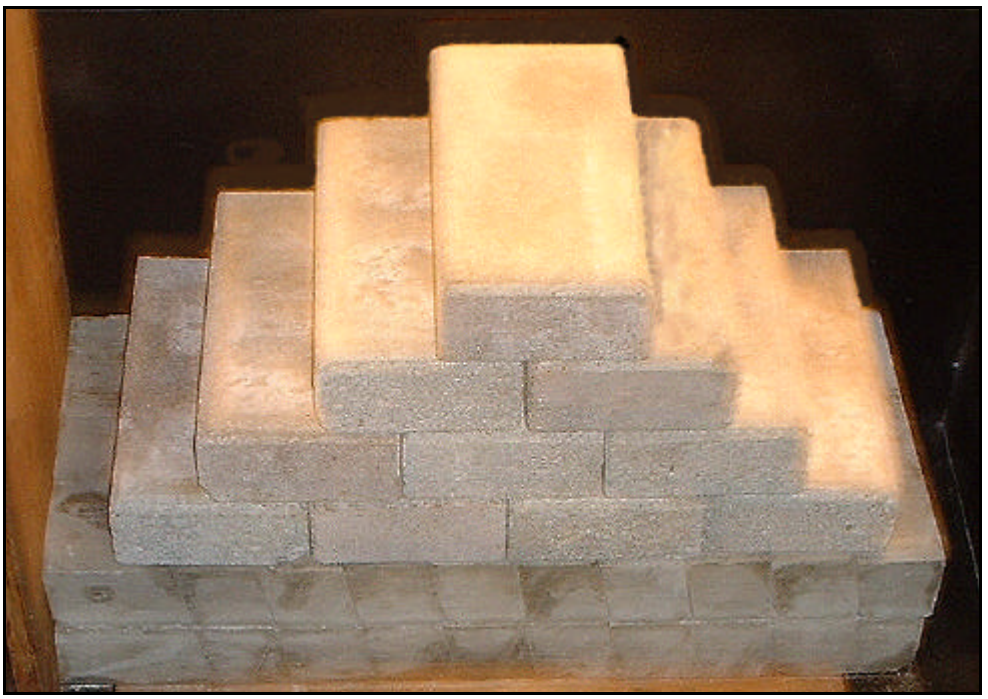

Figure 23. Assembled unbolted model

The “bolts” were pieces of 3 mm diameter standard steel wire. The pieces were inserted in the holes created by the nails. Pratley epoxy was used as “resin” to fix the reinforcement in place. A fully grouted bar was modelled in this way. The free ends of the bolts were bent back until parallel with the underside of the bolted layer. Following installation, the epoxy was left to cure for 90 minutes before the testing procedure began. Figure 24 shows both the layers just prior to testing.

Figure 24. Lower bolted layer and upper unbolted layer

3.2.3. Testing procedure

Figure 19 shows a conceptual illustration of the test setup. In practice, the setup begins with the placement of a board between the ledges in the test frame. This board is supported by a hydraulic jack which is pumped up so that the board is at the level of the ledges. Another board is placed against the vertical wall of the frame and the blocks are assembled against this board and on top of the supporting board. Figure 25 shows the assembled model at this stage.

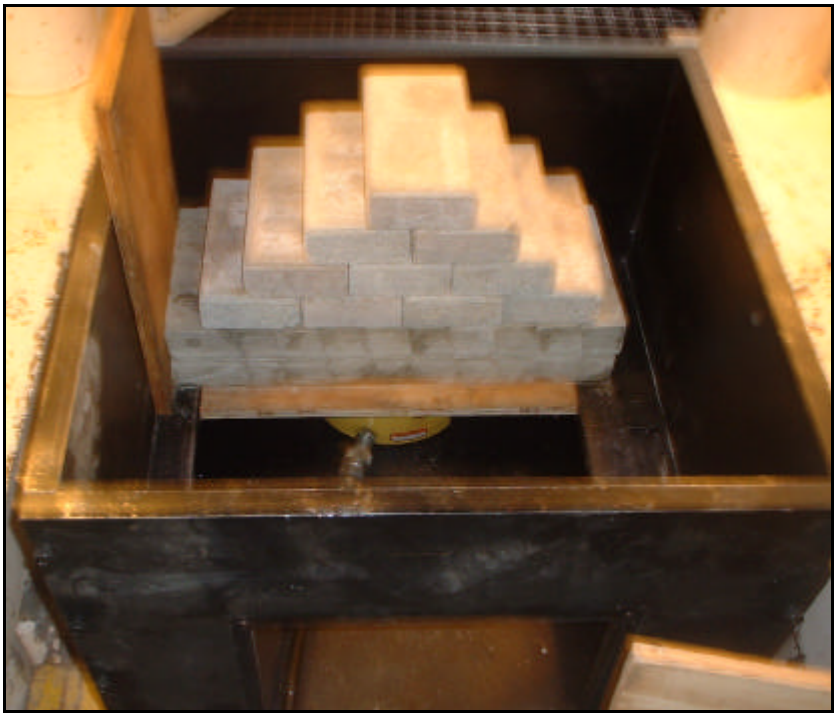

Figure 25. Model assembly

Figure 26 shows a top view of the assembled model. Confinement is supplied in both horizontal directions. Loads perpendicular to the discontinuities are applied via the Vetter Bag, which is capable of applying 150 kN at 800 kPa air pressure. The bag was inflated to a 6 bar pressure for the test. The area over which this load was applied is not easily determined, as the surface of the bag overlapped the loading platen somewhat. The inflated “pillow” shape of the bag also results in an uneven load distribution. It is estimated that the resultant load on the model was between 16 kN and 24 kN (0.73 MPa to 1.09 MPa). A hydraulic jack pressing against a steel plate was used to supply confinement in the opposite direction. The jack was extended until a 3 MPa pressure was recorded, which corresponds to a load of approximately 21 kN (0.72 MPa). Steel platens were placed between the concrete blocks and the loading devices.

A spherical seat is installed on top of the model to ensure good contact between the loading piston and the model. The Terratek piston is moved down so that it makes contact with the uppermost brick and the confining loads are applied. Once the confinement has been applied, the jack underneath the model is released and removed along with the supporting board. At this point the concrete blocks must remain in place for the testing procedure to continue. Figure 27 shows the fully assembled test. The white object between the spherical seat and the Terratek piston is a piece of paper used to check whether contact between the piston and the model was established. Note that the displacement quoted is the displacement of the Terratek piston and is not necessarily the same as the flexing beam at the base of the model.

The procedure was essentially the same for the bolted and unbolted models, though the bottom layer in the bolted model essentially became one block once the bolts had been glued in.

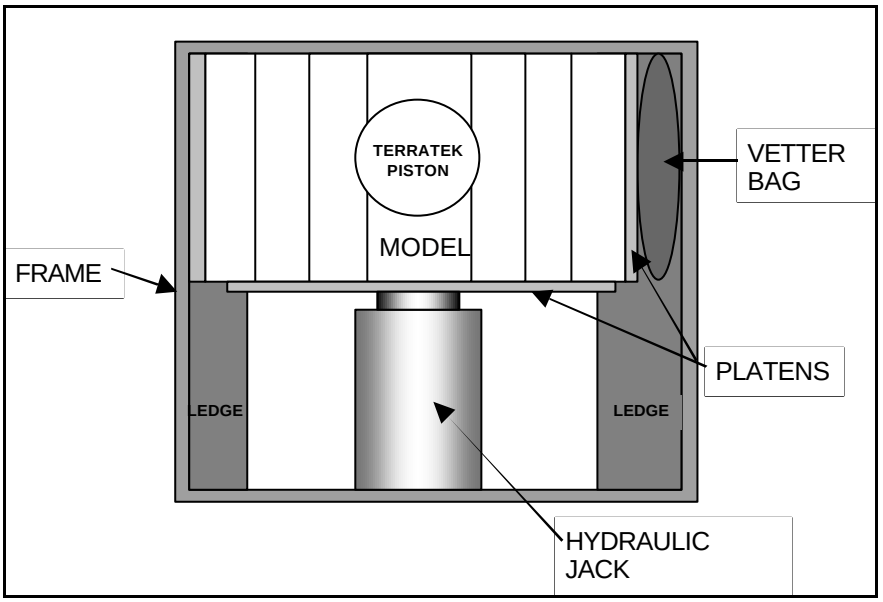

Figure 26. Top view of the test setup

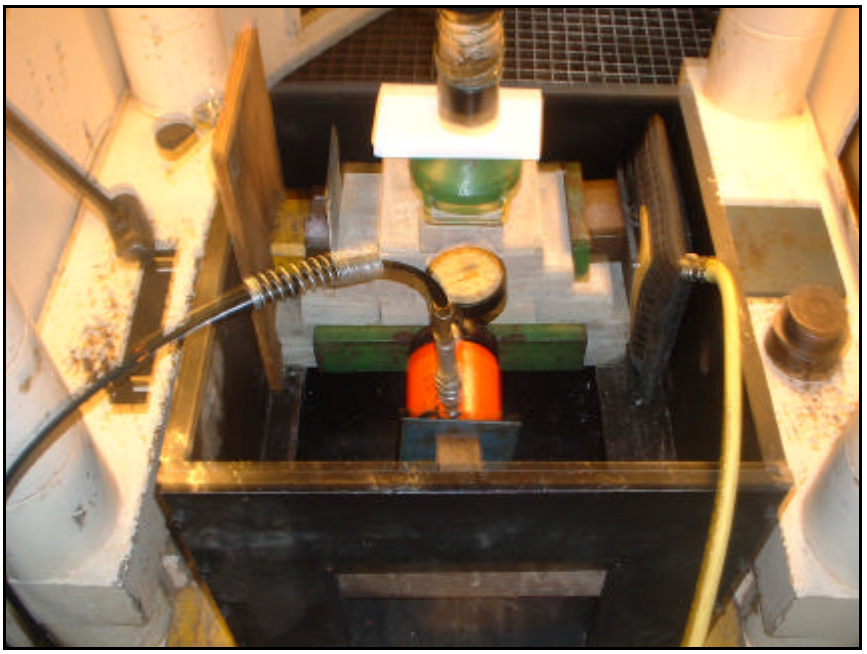

Figure 27. Fully assembled model with confining loads applied

3.3. Results

The results are expressed in terms of vertical load vs. vertical displacement curves for the beam. Such curves indicate both the stiffness and strength of the beam, and the energy-absorbing capacity of the system. Photographs were also taken during the test to indicate beam flexure and the state of the concrete blocks.

The load–displacement curves for the two models are presented in Figure 28. The approximate strength of the unbolted model is 20 kN and for the bolted model, 90 kN, indicating an increase in strength of 450 %. The individual curves are examined in more detail with the aid of photographs, taken at various stages of loading and deflection.

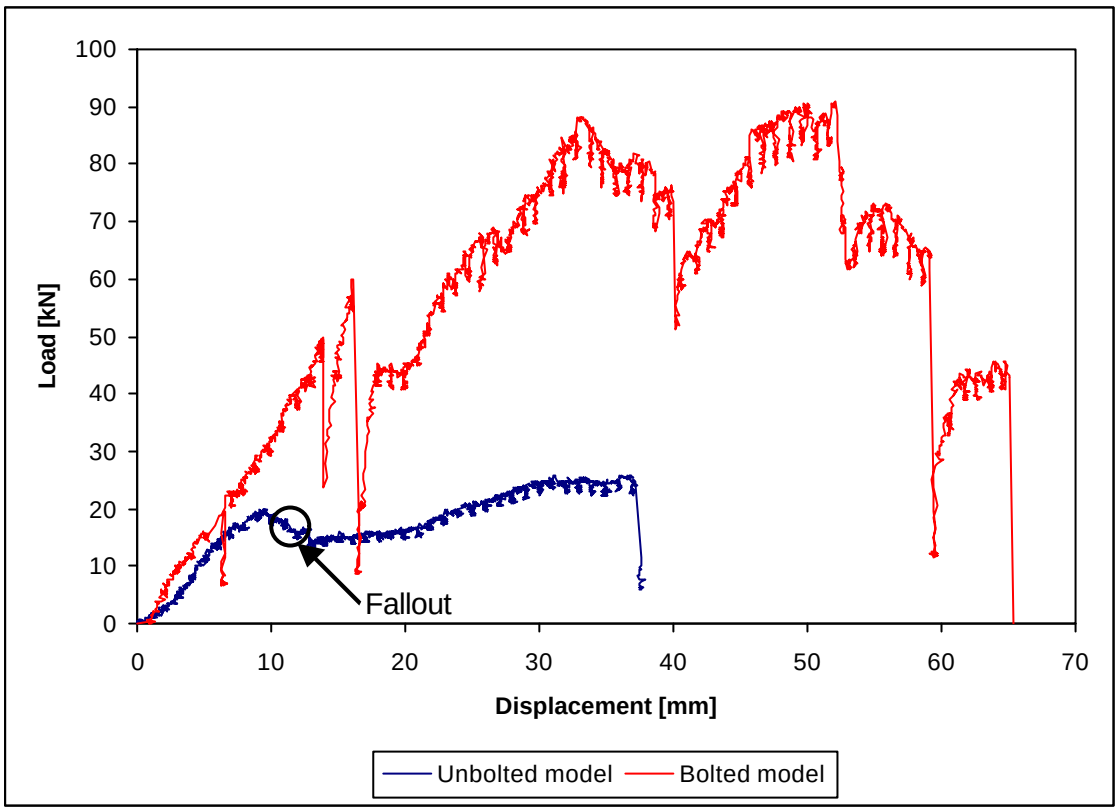

Figure 28. Load–displacement curves for the bolted and unbolted models

3.3.1. Unbolted model results

The unbolted model was successfully suspended by confining forces only. After an approximately 8 mm displacement, cracking was observed in the outer block (supported on the steel ledge) in the lower layer. Figure 29 shows the model after approximately 23 mm displacement. The crack had by this stage fully developed and is circled. After a 10 mm displacement was reached, cracking of the concrete bricks above the model was observed (also circled in Figure 29).

At approximately a 12 mm displacement, most blocks of the lower layer fell out. The drop in load at this point is indicated in Figure 28. The shape of the beam before and after this event is illustrated in Figure 30. The test was continued until it seemed that a constant load had been achieved. The bricks and remaining concrete blocks showed significant damage at this point and it was believed that the strengths of the materials were now being tested rather than the integrity of the beam. The test was stopped and the Terratek piston retracted, at which point the entire model collapsed as the confining stresses imposed by the Vetter Bag suddenly forced blocks both upwards and downwards. The bag was fully inflated and unloaded following the collapse.

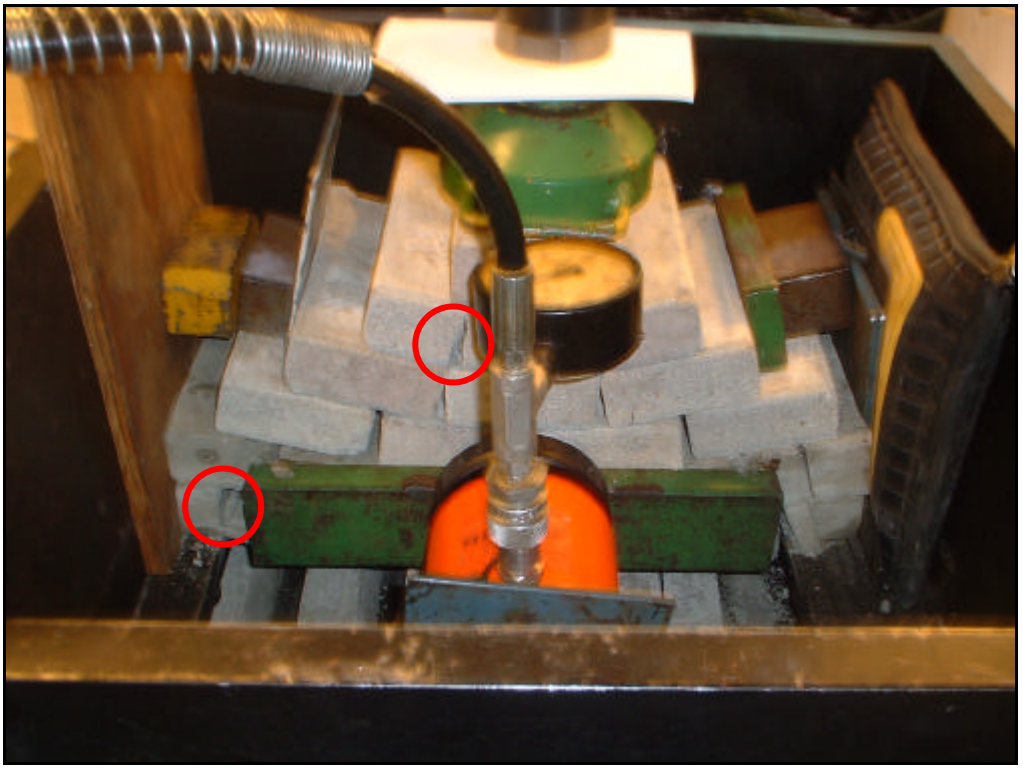

Figure 29. Full view of the unbolted model test

Figure 30. Underside of the beam before and after fallout

3.3.2. Bolted model results

The beam was suspended by confining stresses, only with no initial flexure. Photographs of the beam were taken at 5 mm intervals – all of these pictures are presented in Figure 31. The main part of the lower layer remained intact throughout the test. Cracking of concrete at the ledge contact was observed - Figure 32. Failure of the load-spreading bricks was also evident. The large load drops in Figure 28 may be attributed to these failures. Figure 31 shows how the integrity of the lower layer was maintained throughout, despite cracking on the ledges. It is also notable that a large separation between the layers occurred at high displacements. This was cause primarily by the cracking at the edges, as this allowed a large rotation of the ends of the beam. This can be seen quite clearly in the second part of Figure 32 – the mount of rotation permitted by the fully developed crack in the lower layer is much greater than that of the partially cracked upper layer.

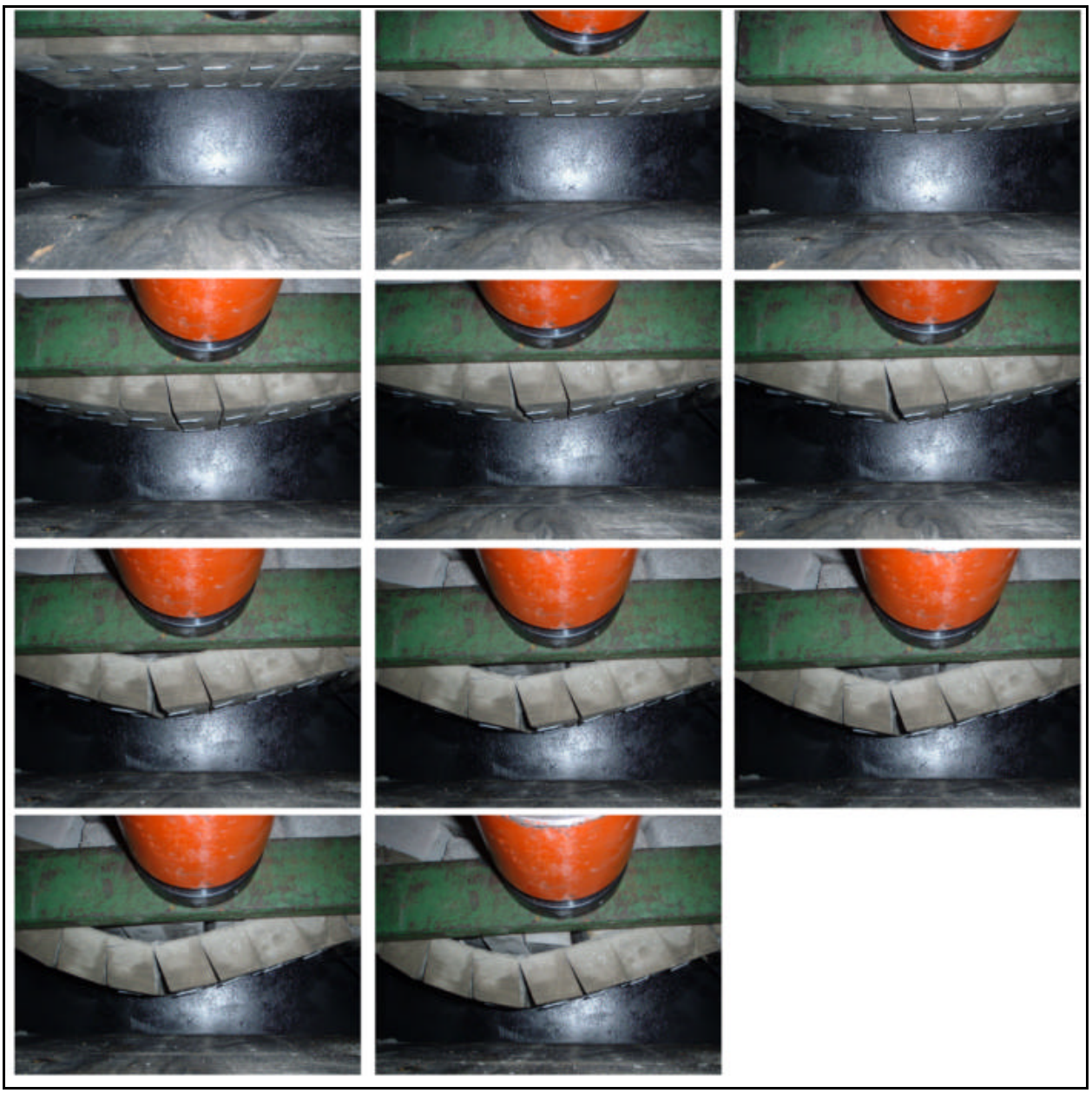

Figure 31. Beam photographs at 5 mm displacement intervals for the bolted model

The test was stopped after the model collapsed. Rotation of the supporting blocks resulted in a sudden loss of confinement which caused the model to fail. The final state of the model with all loading apparatus removed is presented in Figure 33. Note that the bolted layer still provides support on the left-hand side. Most of the bolted layer was intact and could be removed in one piece. Blocks that had broken at the ledge contacts had obviously separated. Bond failure was observed in many of the bolts. A significant number of pull-out-type partial failures was observed.

Figure 32. Progression of cracks in concrete blocks

Figure 33. Final state of the bolted model

3.4. Discussion

The lab tests have shown that even the presence of short bolts can have a significant strengthening effect on the hangingwall beam. By increasing the integrity of the immediate hangingwall layer, the strength, stiffness and energy-absorbing capacity of the system is increased. For the geometry modelled, the following improvements were obtained:

Table 2. Comparison of laboratory tests with and without bolts

Result	Unbolted model result	Bolted model result	Improvement [%]
Strength [kN]	19.5	90.5	464
Initial stiffness [kN/m]	2234	3072	137
Energy absorbed [kJ]	5.5	13.7	249

The initial stiffness is calculated by measuring the slope of the curve from the start of the test until clear deviation from linearity is observed. The energy absorbed was calculated by integrating the load-displacement curve. Only the first 37.5 mm of displacement was considered as the unbolted test was stopped at this point.

While the improvement with bolting is clear, a number of issues were raised in evaluating the testing procedure, possibly influencing the quantitative improvements.

- The strength of the bolts was exaggerated
    - While failure of the bond and "pulling out" of bolts was observed, it is agreed that the 3 mm diameter bolts were too strong to simulate the failure characteristics of scaled-down full-column grouted bars.
    - Scaling of the bolt diameter should therefore primarily consider the bolt strength, bond strength and yieldability.

- Application of in-plane confinement could be improved
    - The platen used between the model and the hydraulic jack did not cover the entire side of the model, resulting in localisation of the confinement. This may have effected the unbolted model result in particular, as fallout was observed shortly after the central block had lost contact with the platen.
    - Downward movement of the platen was observed. Though this does not have serious implications in terms of the results, it does indicate a small loss of energy from the system.
    - A large, fully supported platen will alleviate these problems.

- Differential support resistances should be used
    - The support for the beam was supplied at both ends by steel ledges. It is proposed that different supports should be used at either end to simulate the effect of the face and the back area support.
    - This can be achieved by using different materials with scaled-down properties which approximate the support resistance supplied by the back area and the face.

- Fracturing of the concrete blocks introduced unknown parameters into the system
    - Not only is the effect of this non-linear behaviour unquantifiable, it makes calibration of equivalent numerical models very difficult.
    - Use of softer end supports may alleviate this problem. The magnitude of the confining stresses may also be a factor.

The testing procedure can be applied to any hangingwall geometry, though it should be pointed out that these tests are extremely time consuming. The main difficulty is in creating the concrete blocks, as the construction of the moulds becomes very complicated when intersecting discontinuities are considered. The test setup is also a cumbersome affair, as various spacers, shims and plates are required to ensure a good fit between blocks and platens. The Vetter Bag is also not ideal for the purpose of applying the confining stress, as bulging of the bag results in irregular loading and it becomes difficult to estimate the applied load and its distribution through the model.

4. Numerical modelling

Modelling was conducted using the ELFEN numerical modelling suite. ELFEN is a finite/discrete element code which allows for full contact interaction between multiple deformable bodies. The explicit time integration algorithm (similar to the algorithm employed in FLAC and UDEC) inherently includes capability for dynamic deformations and loadings. The algorithm also allows for simple and stable execution of non-linear material models.

The model may be constructed in much the same way as a physical model. The geometry is defined using a CAD-type interface and constraints and loadings are then applied to geometric entities. A control is applied to define the time curves for the loads and to specify different stages for the analysis. An advancing-front mesh generator is invoked and the geometry is discretised (in this case) into 2D triangles. The model is then analysed.

4.1. Analysis schedule

A model representing the laboratory tests was first constructed. This model is scaled-down as in the laboratory and attempts to reproduce the results obtained in the laboratory with and without bolts. The main aim was to obtain comparative results. To reproduce the results quantitatively would be very difficult owing to the various unknown quantities (contact properties), and because of non-linear behaviour (cracking) of the blocks in the laboratory tests.

The three generic hangingwall types identified in the literature survey were modelled. Geometric and contact parameters in each of these models were varied. The model loading and boundary conditions are essentially the same as those employed in the laboratory tests. The models are effectively tests of hangingwall integrity with applied confinement and an increasing vertical load.

4.2. Modelling of laboratory tests

The numerical model is geometrically identical to the laboratory model. The model is illustrated in Figure 34. Face loads are applied where the Vetter Bag is inflated and displacement loads are applied vertically to simulate the Terratek piston. The bricks and concrete blocks are assigned generic concrete properties, as presented in Table 3. The platen between the bag (face loads) and the model is assigned downgraded properties to account for deformation of the bag. All other solids are assigned the properties of elastic steel. Note that a steel plate is included behind the position of the Vetter Bag. This is to simulate the confinement created when the bag is pushed against the side of the test frame by lateral movement of the concrete blocks.

The bolts (indicated in Figure 34) are assigned the properties of elastic steel, with a diameter of 3 mm.

Table 3. Elastic material properties for the laboratory test model

Material	Young's modulus [GPa]	Poisson's ratio	Density [kg/m^3]
Concrete blocks	30	0.2	2500
Bricks	30	0.2	2500
Steel	200	0.3	7860
Bag platen	10	0.2	2500

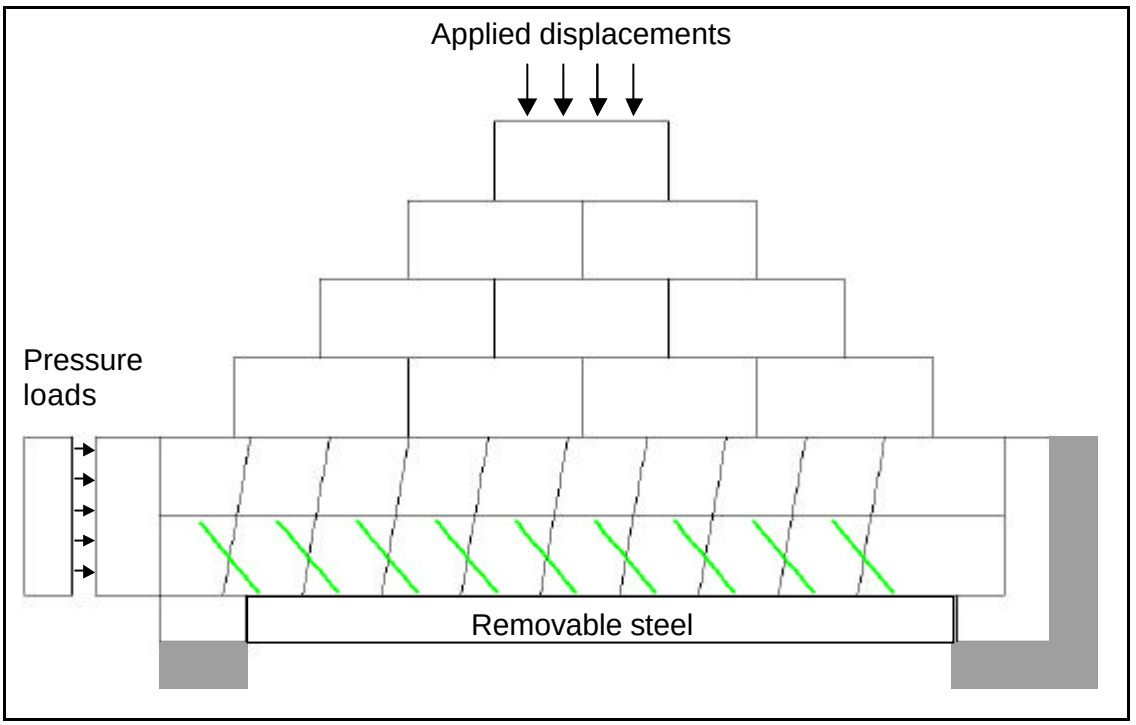

Figure 34. Numerical model of the laboratory test setup

The analysis is run in two stages. In the first stage, the horizontal face load is applied and gravitational acceleration is activated throughout the model. During this stage the removable steel block indicated is present, just as a supporting board and jack was used in the laboratory model. Once dynamic relaxation has occurred and the velocities in the system have decreased to a negligible level, the removable steel is deactivated, allowing the concrete beam to flex freely. A short period of dynamic relaxation follows. The vertical displacement loads are then applied, ramped linearly over time to 50 mm displacement.

4.2.1. Results

The load-displacement curves for the two models are presented in Figure 35. The shape of the unbolted curve is remarkably similar to that of the laboratory test result, though quantitatively the magnitudes are up to two times greater in the numerical result. The bolted model result does show an increase in stiffness and strength, though not to the degree found in the laboratory. An 87% increase in strength (if the unbolted model strength is taken as maximum before the first load drop) is observed with the inclusion of bolts. An increase in stiffness of 54% is also observed.

Figure 36 and Figure 37 show the final states of the unbolted and bolted models respectively. The loss of contact in the bottom layer of the unbolted model indicates that the beam is fully unstable and about to fall freely. The bottom layer of the bolted model is still intact and very similar to the final beam shape observed in the laboratory – see Figure 31. Of note are the bending/shear deformations of the bolts. Judging from the photographs, shearing deformation could initiate after about 30 mm, which corresponds to 0.3 m closure in the full-scale stope. This could indicate a shear deformation requirement for bolts in the face area, particularly for more complicated rock mass block geometries.

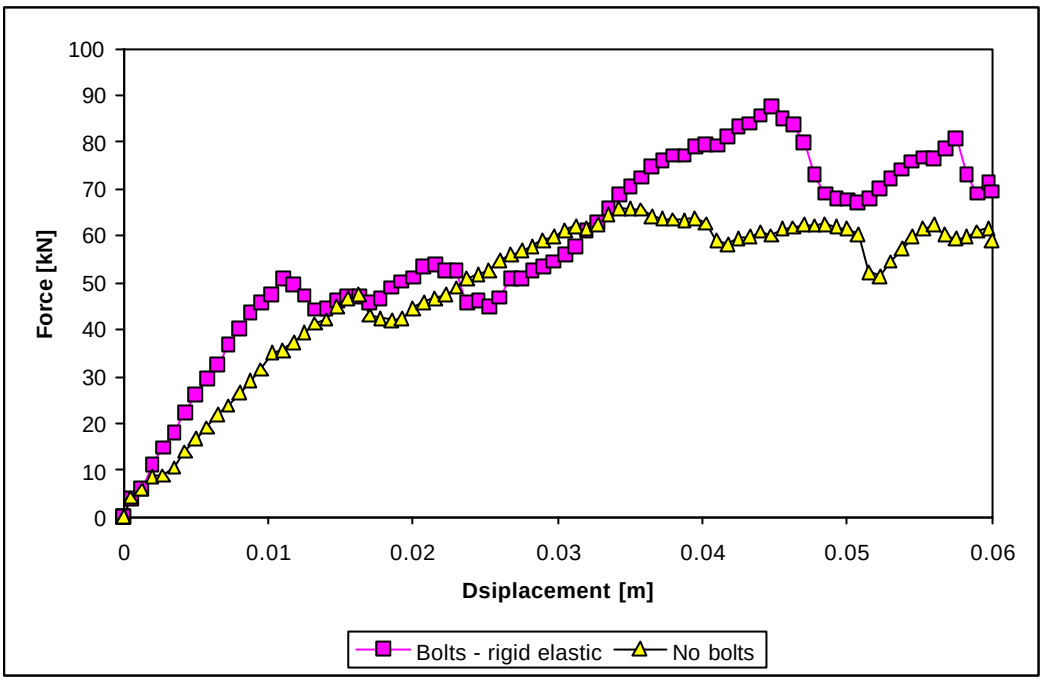

Figure 35. Load-displacement curves of numerical models of lab tests

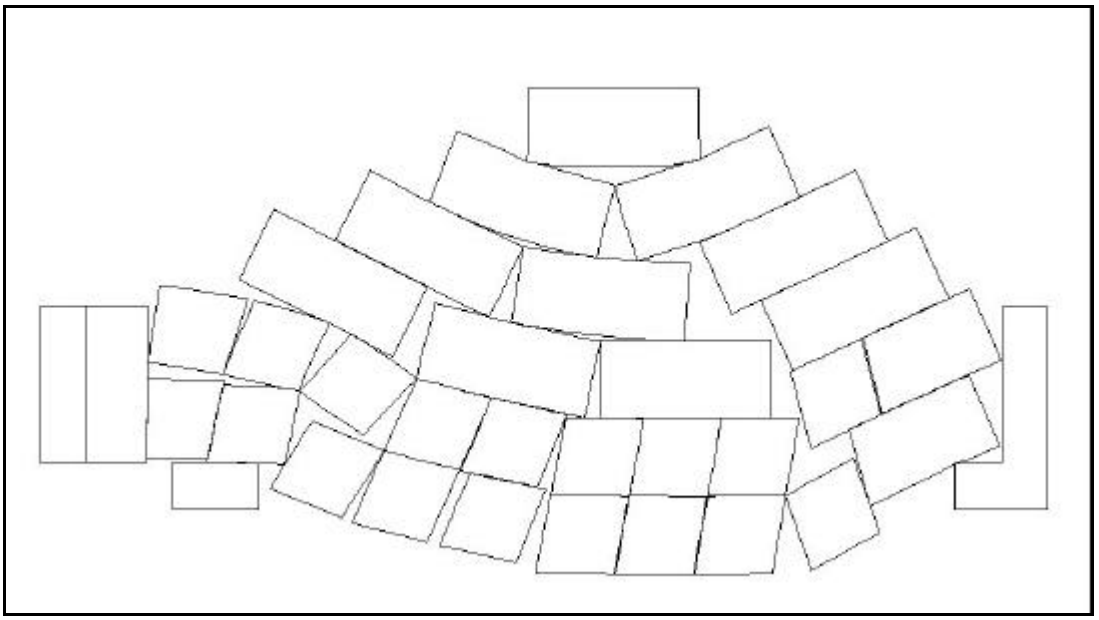

Figure 36. Final state of the unbolted numerical model

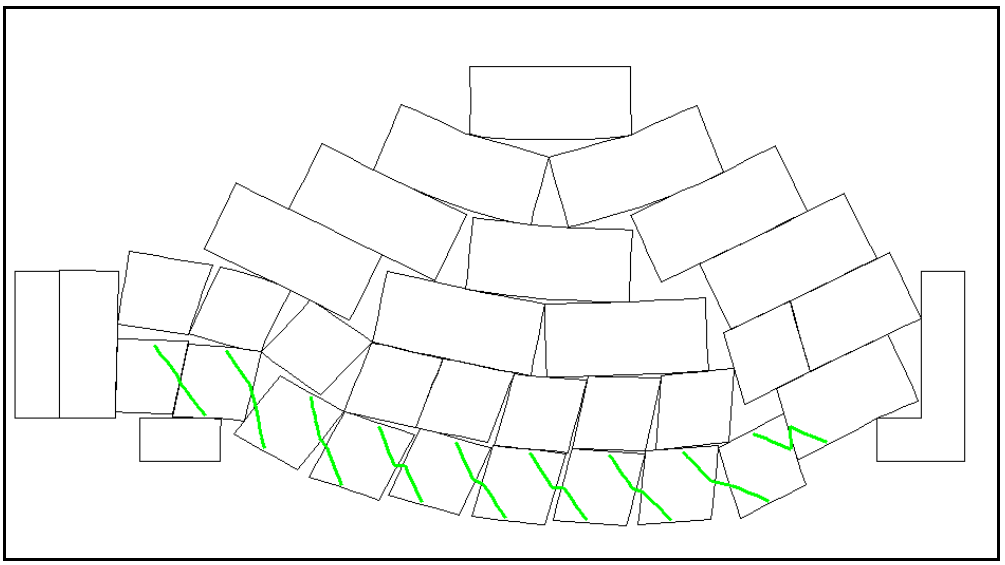

Figure 37. Final state of the bolted numerical model

4.3. Modelling of generic hangingwall types

The template for all these models is illustrated in Figure 38. The hangingwall is a 3 m by 6 m section made up of discrete blocks created by the jointing or fracture pattern. Discrete rectangular “bricks” are stacked on top of the hangingwall section in the shape of pyramid. This pyramid ensures that load is spread out at (at least) a 45^0 angle. Displacement loads are applied to the top surface of the uppermost brick, as illustrated. Horizontal confining pressure loads are applied via a loading platen. A fixed platen on the opposite side of the model allows confining stress to build up in the hangingwall section.

The hangingwall is supported by three blocks, two of these representing the back area (permanent support) and the face. The other block provides initial support and is removed after the horizontal confining stresses are fully applied. The analysis is conducted in two stages with load-curves defined appropriately. In the first stage, the confining forces and gravity acceleration are applied. After the forces are fully applied, an idle period follows during which dynamic relaxation reduces velocities to negligible values. The removable support is then deactivated and the vertical displacement loads are applied.

Bolts are 0.8 m in length and are assigned a diameter of 16 mm. They are “rigidly coupled” to the continuum elements, meaning that the displacement of individual bolt elements is equal to the relative displacement between ends of the element. The bolts are also linear elastic with no capacity for failure or yielding. The bolting patterns for the generic hangingwalls obey the practical and economic limitations imposed in a typical gold-mining production cycle. The bolts are installed at approximately 0.5 m behind the face, and are spaced 0.8 m to 1 m apart in the direction of mining. The relationship between observed fracture/joint orientations and spacing, and the chosen bolt pattern, is quite arbitrary. Only the bolt orientations are adjusted to suit the dominant discontinuity sets. Orientations were obtained from personal communication with staff working on guidelines for stope face bolting practices. No spot-bolting is applied.

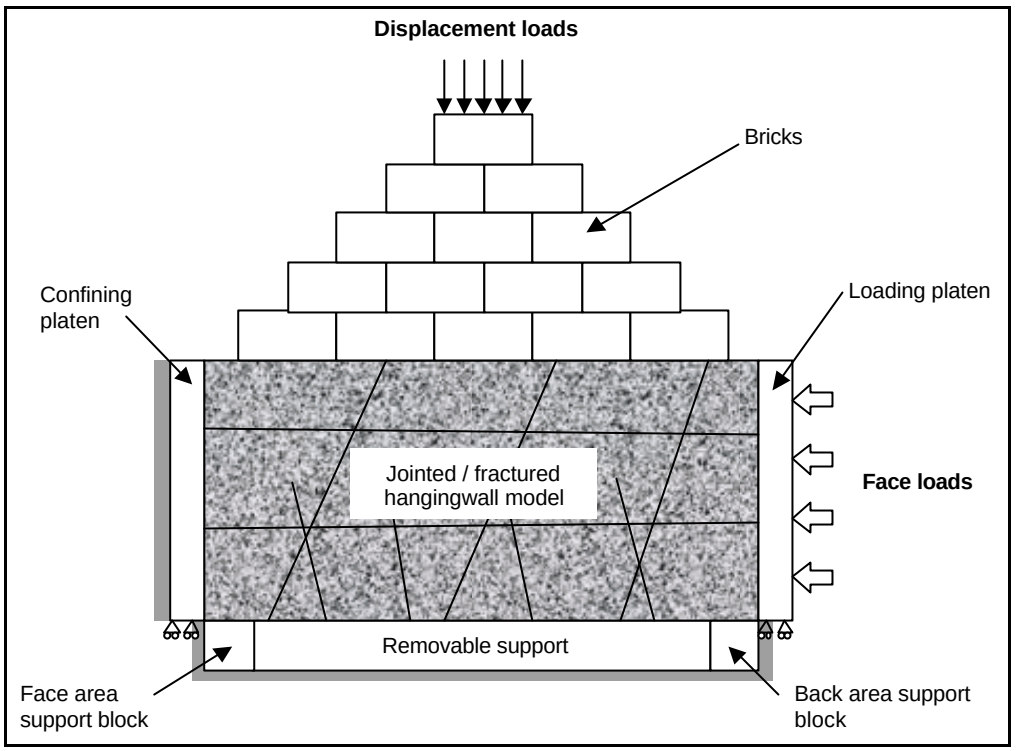

Figure 38. General numerical model geometry

4.3.1. VCR model description

The VCR hangingwall is characterised by jointing and extension fractures. The spacing and orientation of the jointing is site-specific and can be arbitrarily selected based on personal experience (Roberts, 2001). The extension fracturing is assumed to be similar to that observed at all deep-level stopes – oriented at approximately 80^0 and spaced between 0.05 m and 0.5 m. The following joint and fracture parameters were selected for the model:

Table 4. Discontinuity sets for the VCR model

Discontinuity set	Orientation from positive horizontal	Spacing [m]
Joint set 1	30	1.5
Joint set 2	135	1.4
Extension fractures	100	0.5

The VCR model geometry is illustrated in Figure 39. Bolt positions are indicated. Bolt orientation is vertical.

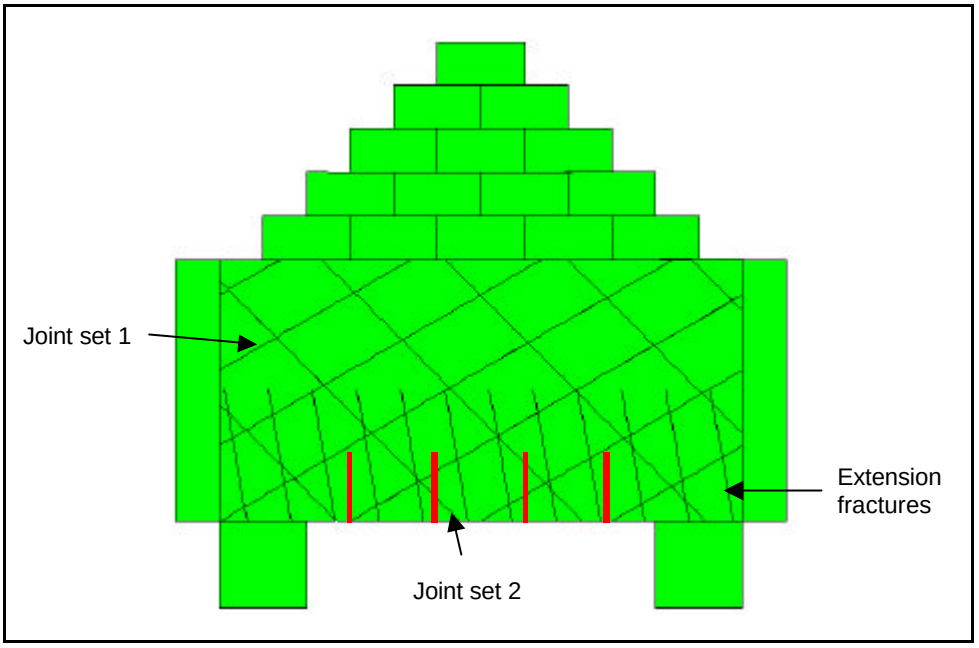

Figure 39. VCR model geometry

4.3.2. Results from the VCR model

The load-displacement curves from the bolted and unbolted models are presented in Figure 40. The curves are very similar in nature, and an 8.8% increase in strength is indicated with bolts present. Examination of the hangingwall at termination of the analysis shows why the results are so similar. The failure mode of the unbolted model (Figure 41) is primarily by slipping and separation along the joint indicated. Much of the hangingwall to the left of this plane is intact and falls together. Exactly the same failure mode is observed in the bolted model (Figure 42).

The position of the “rightmost” bolt is crucial to preventing failure of this beam. With the arbitrarily selected bolting pattern, that bolt is positioned within a solid block and therefore contributes nothing towards the integrity or strength of the beam. The (slight) increase in strength with bolting is due to increased integrity of the remaining portion of the hangingwall. A greater load is required to mobilise the displacements which ultimately lead to failure along the main joint.

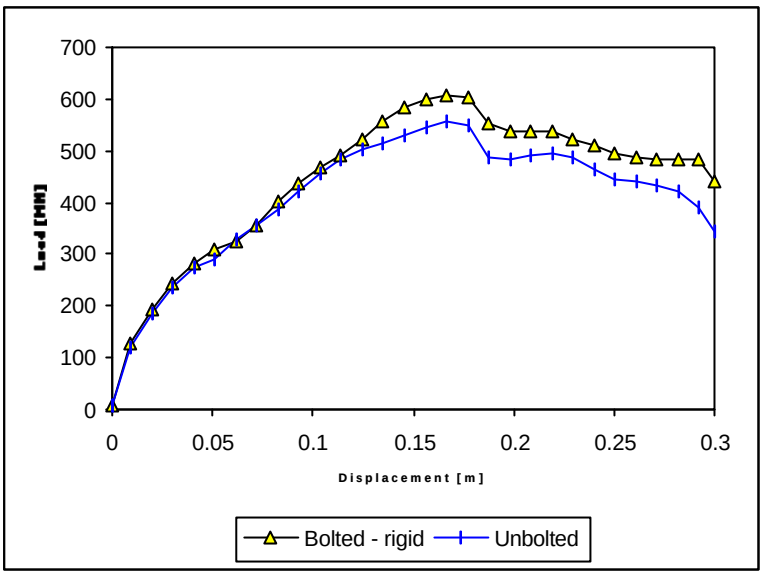

Figure 40. Load–displacement curves for the VCR model with and without bolts

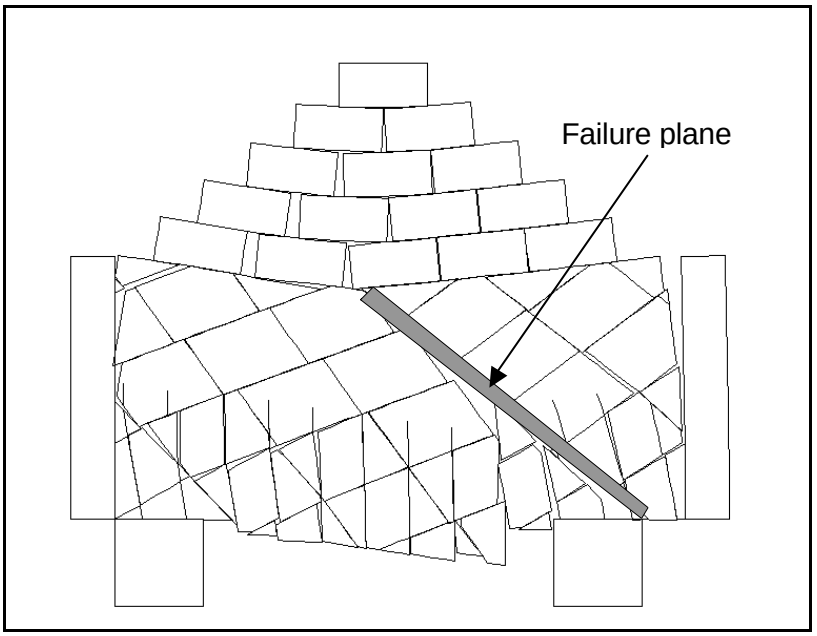

Figure 41. Final state of the unbolted model

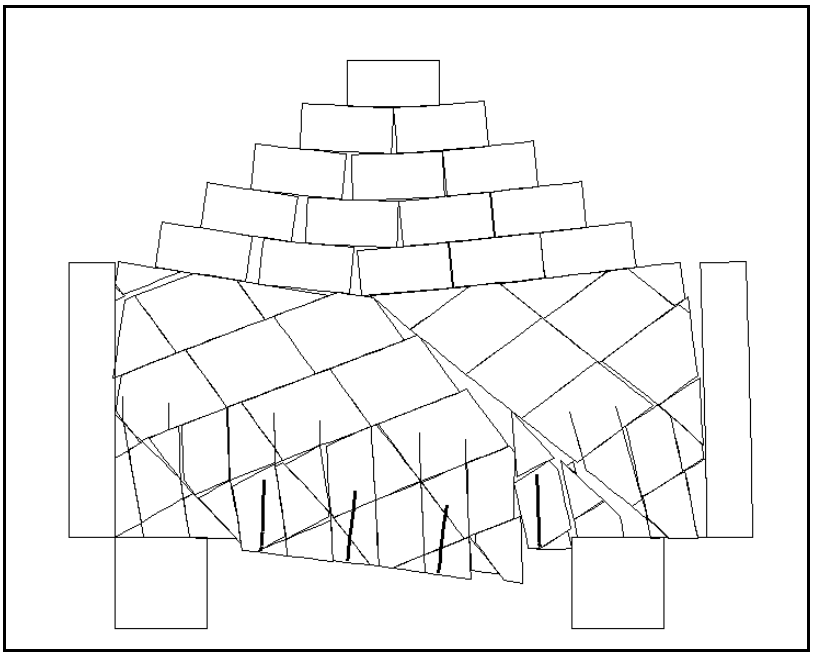

Figure 42. Final state of the bolted model

4.3.3. Carbon Leader model description

The Carbon Leader generic hangingwall is characterised by the presence of the Carbon Leader beam, typically 1.8 m – 2.0 m above the hangingwall contact. Also present are extension fractures, shear fractures and low-angle fracturing. The Carbon Leader contacts in the numerical model are at 1.8 m and 2.2 m above the hangingwall contact. The other fracture sets have the following characteristics.

Table 5. Discontinuity sets for the Carbon Leader model

Discontinuity set	Orientation from positive horizontal	Spacing [m]	Vertical extent [m]
Extension fractures	100	0.3	1.8 (to Carbon Leader)
Shear fractures	70	2.0	3.0 (to top of model)
Low-angle fractures	165	0.8	0.6

Bolts are installed at a 60^0 angle. The geometry of the model and the relative positions of the bolts are illustrated in Figure 43.

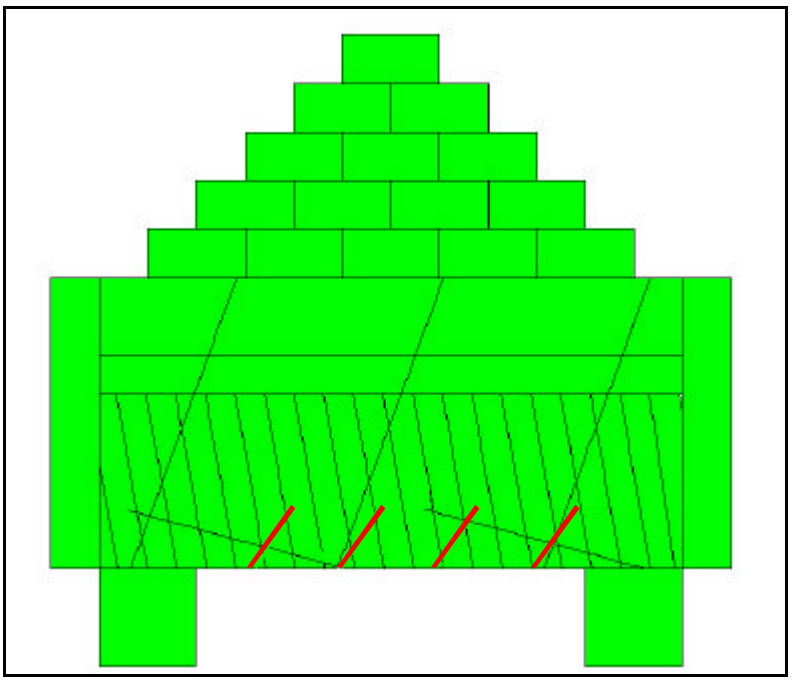

Figure 43. Carbon Leader model geometry

4.3.4. Results from the Carbon Leader model

The load-displacement relationship is presented in Figure 44. The curves show a similar initial stiffness, but the load in the bolted model increases markedly at around 0.1 m displacement. A 22.6% increase in strength is obtained by including bolts. Figure 45 and Figure 46 show the final states of the unbolted and bolted models respectively. A number of failure planes are present in the result, with sliding evident on all discontinuity sets. Comparing these figures, it is evident that the profile of the beam is "flatter" for the bolted model. Bolts traversing the low-angle fractures and extension fractures have limited the displacement between adjacent blocks, thus reducing the potential for instability. The unstable region at the face side of the beam has been stabilised by the rightmost bolt.

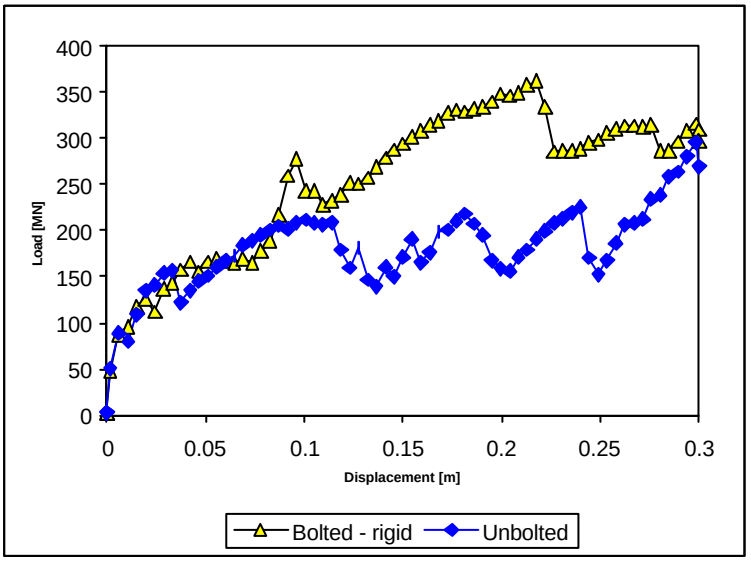

Figure 44. Load–displacement curves for the Carbon Leader model with and without bolts

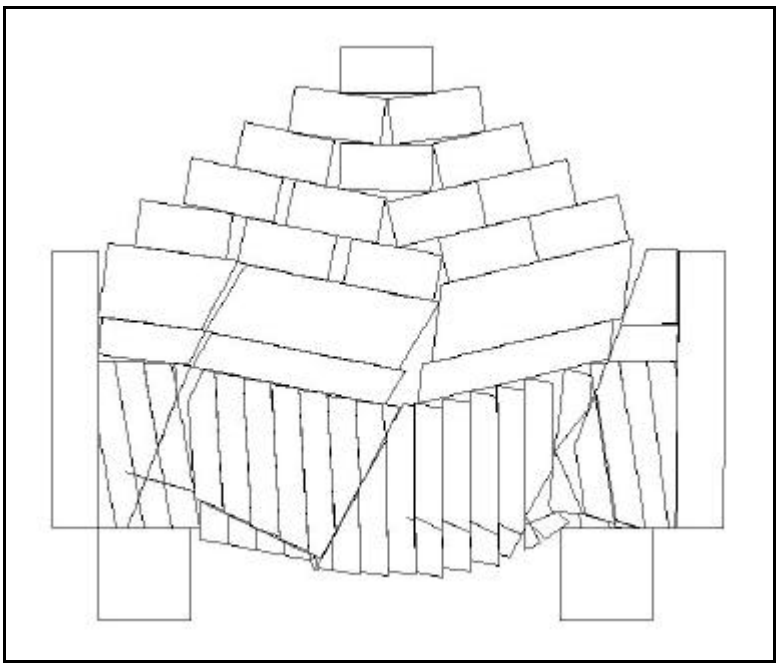

Figure 45. Final state of the unbolted Carbon Leader model

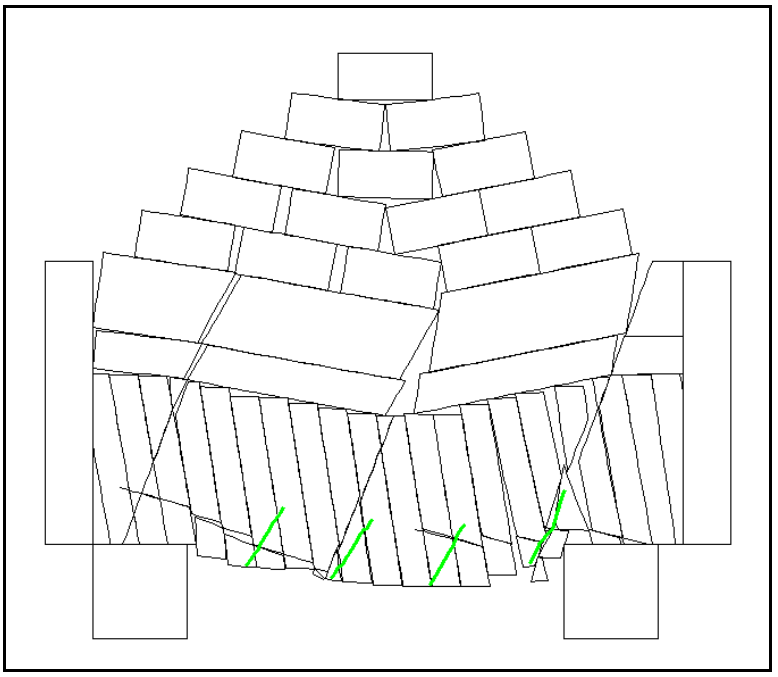

Figure 46. Final state of the bolted Carbon Leader model

4.3.5. Vaal Reefs model description

The Vaal Reefs generic hangingwall is regularly bedded at a spacing of between 0.3 m to 0.6 m. Extension fractures and shear fractures are also present. For the numerical model, the bedding is spaced at 0.3 m and the fracture sets have the following characteristics:

Table 6. Discontinuity sets for the Carbon Leader model

Discontinuity set	Orientation from positive horizontal	Spacing [m]
Extension fractures	100	0.53
Shear fractures	70	2.1

Figure 47 shows the model geometry and bolt positions.

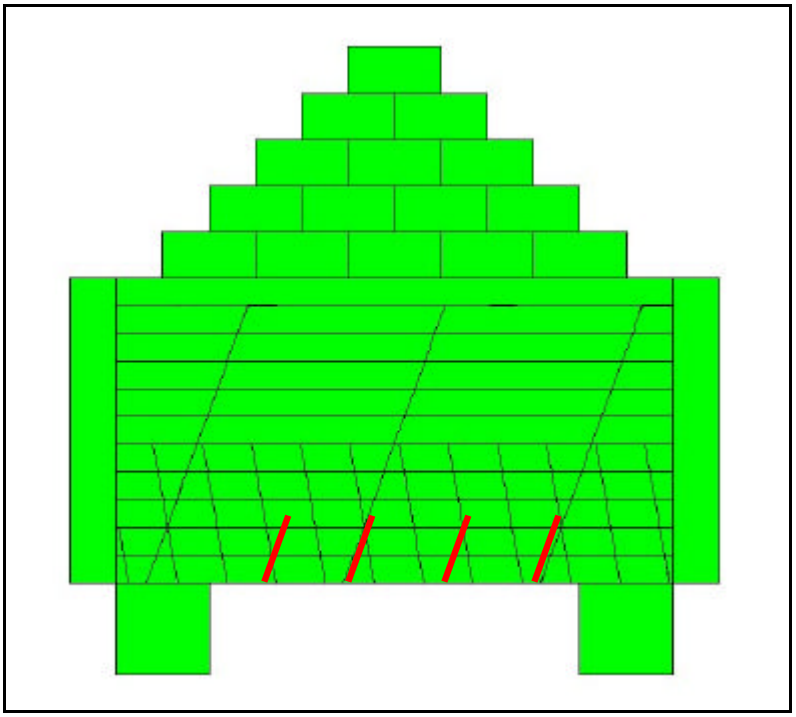

Figure 47. Vaal Reefs model geometry

4.3.6. Results from the Vaal Reefs model

The load-displacement curve is presented in Figure 48. The response with and without bolts is very similar, with the bolted model giving a 4% increase in beam strength. Deformed geometry plots show why the bolts have had so little influence. Figure 49 is the result without bolts – failure planes have developed along the shear fractures and along the extension fracture overlying the back area and at the face. Figure 50 shows the final state with bolts – note that none of the failure planes have been intersected by bolts, hence the minimal increase in strength.

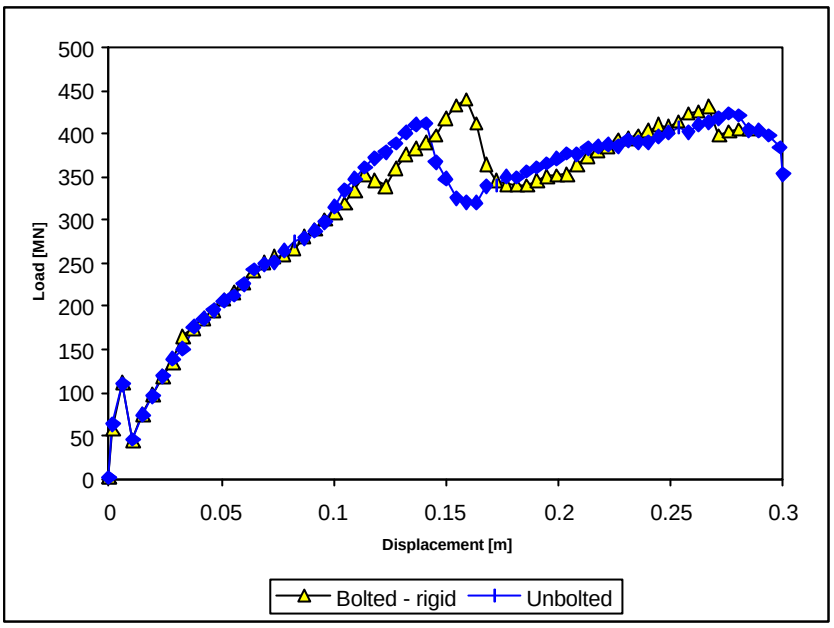

Figure 48. Load–displacement curves for the Vaal Reefs model with and without bolts

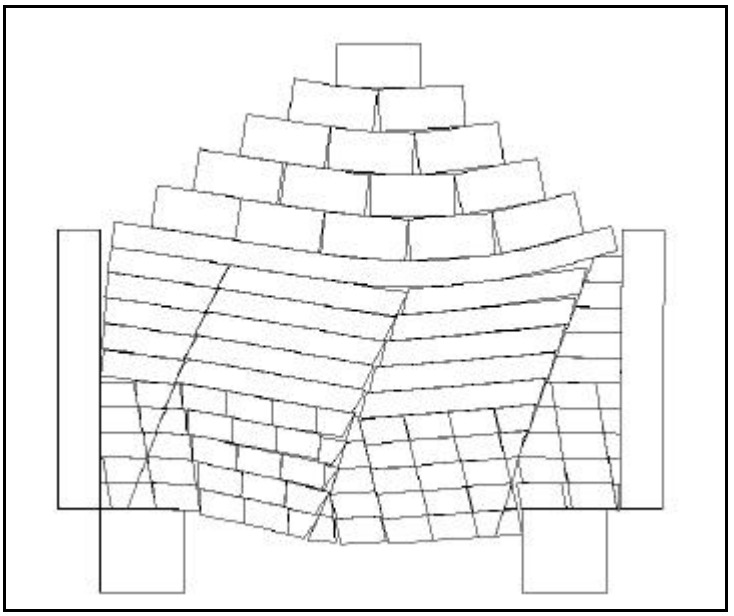

Figure 49. Final state of the unbolted Vaal Reefs model

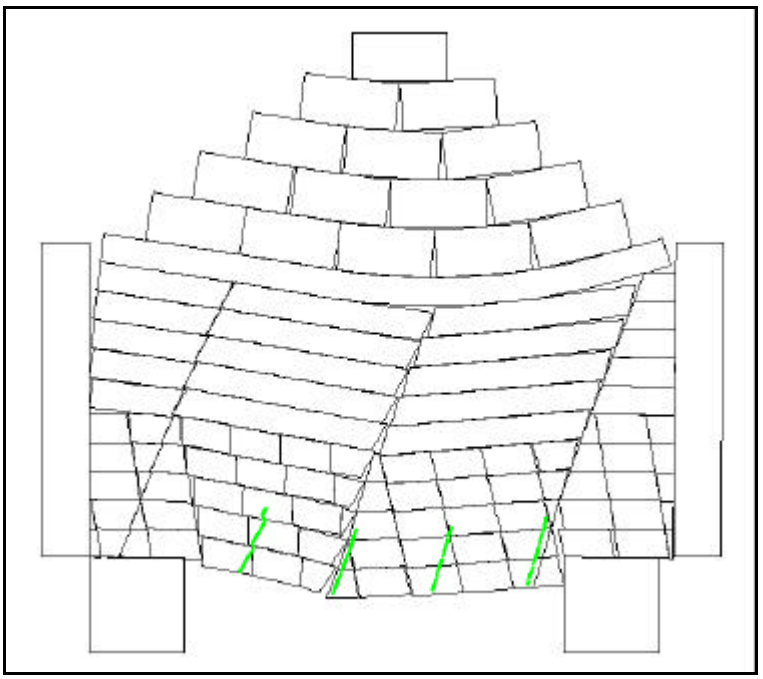

Figure 50. Final state of the bolted Vaal Reefs model

4.3.7. Non-linear rockbolt modelling

As noted above, all models were run with bolt nodes rigidly coupled to the rockmass elements. This means that displacements of the rockmass are directly transferred to the rockbolt, resolved in terms of the orientation of the bolt elements, and expressed as axial displacements along the length of the bolt. These bolts effectively model a full-column grouted bar with an infinitely stiff bond modulus and strength.

A more realistic model takes into account the relative displacements between bar, grout and rockmass that characterise the operation of grouted rockbolts. Such models are available in ELFEN and were used to reinforce the generic hangingwall types described above. The behaviour of such rockbolts is fully determined by the bar material properties and the bond properties. Non-linear models are used to simulate bond and bar yield and failure. A simple strain-hardening model is employed in the case of the bar, with failure at a specified strain. A peak-residual model is employed to describe the behaviour of the bond. This model is illustrated in Figure 51.

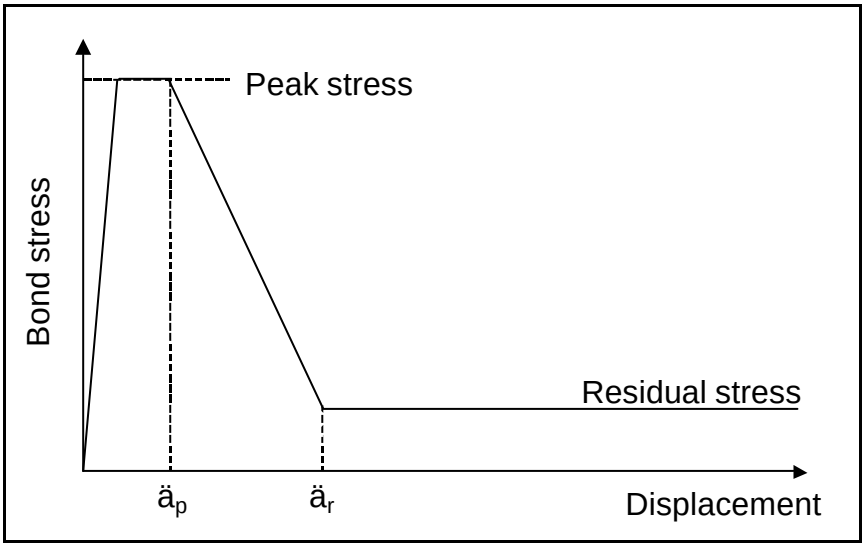

Figure 51. Peak and residual bond model

The bar properties are as follows:

Elastic modulus:	200 GPa
Yield strength:	500 MPa
Ultimate strength:	700 MPa
Ultimate strain:	0.02
Failure strain:	0.0225

The bond properties are as follows:

Bond stiffness:	25 GPa/m
Peak strength:	8 MPa
Residual strength:	1 MPa
$ä_p$	0.12 mm
$ä_r$	1.5 mm

4.3.7.1. Results with non-linear rockbolts

It should be noted firstly that results for the rigidly bonded bolts indicated stresses in excess of 800 MPa. It was therefore expected that the bolts would fail, or at least yield.

The most significant bolt influence was observed in the Carbon Leader hangingwall model. This model is therefore examined in more detail. The results for the rigid bonding and non-linear material models are presented in Figure 52. Examination of bolt behaviour indicated that yield had occurred in most bar elements between 0.1 m and 0.15 m displacement – this corresponds to a drop in load in the response. Bond elements yielded and were all reduced to residual stress responses by 0.145 m displacement. This is a significant point on the response curve, as the resistance offered by the rockbolts becomes constant from there on.

The response from 0.18 m to 0.3 m indicates that the beam system had not completely failed by the time the analysis was terminated. This is a very interesting and significant observation, as it implies that bolts with a “softer” response may be more effective in increasing the strength and integrity of hangingwall beams.

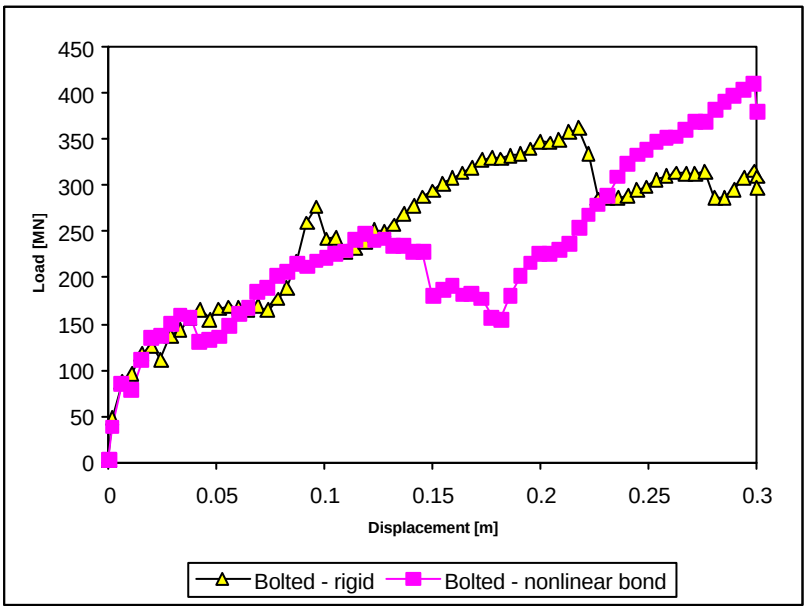

Figure 52. Response for the Carbon Leader hangingwall reinforced with rigidly bonded bolts and with “soft” non-linear bond and material models

4.4. Discussion

Modelling of the laboratory test was relatively accurate in some respects. The form of the load-displacement curve for the unbolted model from the numerical result and from the lab test were very similar. Figure 53 shows the load-displacement relationship for both models. The initial stiffness and the general form of the curve are similar. The higher loads in the numerical model were expected, as no plastic behaviour or cracking of the blocks was permitted. The displacement at peak strength is around 10 mm for the lab test and around 15 mm in the numerical model.

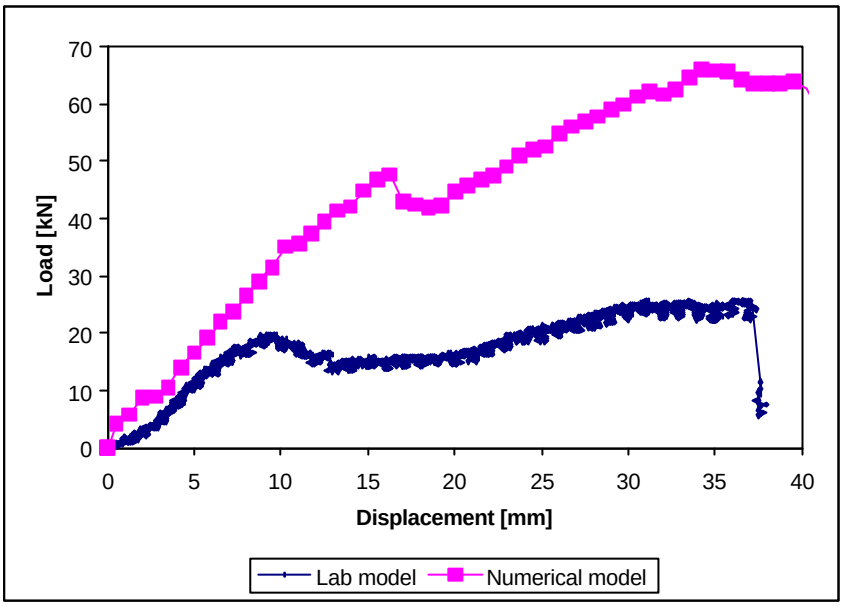

Figure 53. Comparison between the unbolted laboratory and numerical models

The profiles of the bolted beams are also very similar. Figure 54 is a composite picture of the laboratory and numerical results.

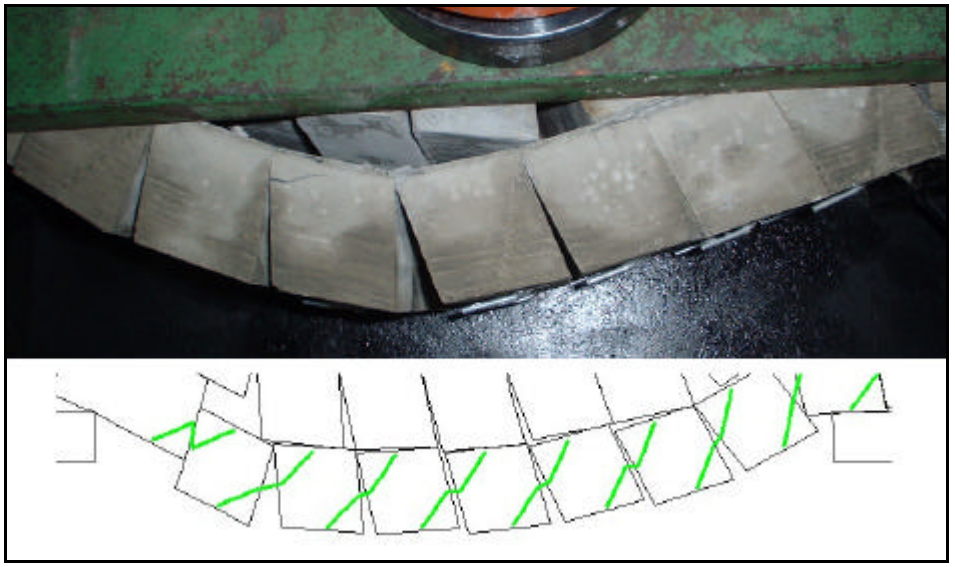

Figure 54. Comparison between laboratory and numerical beam profiles for the bolted model

The indications from qualitative observation are that the results from the models are very similar, however, quantitatively, the bolting showed much less benefit than expected from the

laboratory results. The reasons for the quantitative differences are various – some have been outlined above. Firstly, the blocks in the laboratory model behave plastically and are able to crack, thus effectively altering the geometry of the beam and reducing the stiffness and resistance of the system. Secondly, the bolts as they are modelled only develop stress as a result of axial extension at either end of the beam. Additional resistance from the grout foundation and bending of the steel are not modelled when the bolt is subjected to shear loading. While the axial response does supply a measure of shear resistance as the bolt element elongates across a discontinuity, the direction of the resistance is not exact and the magnitude of the load is under-estimated.

Another possible contributor to the discrepancy is that the out-of-plane stress in the numerical models is related to the sum of the in-plane stress at any point. This is impossible to simulate in the laboratory unless out-of-plane displacements are completely eliminated. With steel platens this can only be partially achieved. The magnitude of the confinement supplied in the laboratory should be calibrated accordingly.

The modelling of generic hangingwalls has shown that bolts do have a beneficial effect in most typical hangingwall geometries, but that the effect is very much dependent on the positions of the bolts relative to the discontinuity sets. The mode of failure of the beam is also important in choosing the most appropriate support pattern. It is interesting to note that most of the generic hangingwall models fail along discontinuities which extend to the top of the model. In practice, this implies that hangingwall failure will occur mostly along shear fractures or persistent subvertical jointing. The bolting pattern should be such that bolts intersect as many discontinuity planes as possible, in particular, those involved in failure of the beam.

The most successful application of bolts was found in the Carbon Leader beam, while the Vaal Reefs geometry showed the least benefit. In the case of the Vaal Reefs model, the bolts did not penetrate any of the discontinuities involved in beam failure. It is suggested that bolting patterns are varied to intersect as many of the overlying discontinuity sets as possible. For example, the orientation of bolts within a single row may be alternated between 60^0, 90^0 and 120^0. If the discontinuities are persistent in the strike direction, then the maximum number of discontinuities will be reinforced.

It was also observed that non-linear bolts with “soft” bonds resulted in a stronger beam than rigidly coupled, perfectly elastic bolts. It is proposed that this phenomenon comes about as a result of the rigidly bonded bolts forcing rotation of blocks within the structure. This leads to redistribution of stresses which may ultimately reduce the load-carrying capacity of the beam. The constant resistance offered by the non-linear bonded bolts will simply reduce the relative displacements between blocks without forcing such rotations. It is imagined that this observation is dependent on hangingwall geometry, the positions of the bolts and the relative values of the nonlinear properties. A full sensitivity analysis is required to determine the relative influences of the controlling parameters.

5. Conclusions and recommendations for further work

The primary finding of this work is that the installation of short bolts can have a beneficial effect on the strength, stiffness and energy absorbing capacity of the stope hangingwall. This finding must be qualified though – the bolting pattern must be such that bolts intersect discontinuity planes involved in failure of the beam. It has been shown in the various generic hangingwall models that failure most often occurs on discontinuities which span the model – whether shear fractures or subvertical jointing. It is suggested that alternating the orientations of bolts in a single row will provide resistance along as many of the discontinuity planes as possible.

The laboratory test showed that bolting can have a major effect on beam strength and stiffness. In the test, the bolts crossed every discontinuity at the most favourable angle, making this

experiment a “best case” scenario. The numerical model of the same test showed the same benefit, but of much lower magnitude. The reasons for this are outlined above.

Various improvements to the lab tests were suggested. The application of the discontinuity-parallel confinement was not uniform. A large plate resting on the ledges and the floor of the apparatus will eliminate this problem. The design and construction of such a plate is a simple matter. The support blocks at the ends of the beam were also identified as being non-representative. These blocks should attempt to model the stiffness of the face and back area, scaled down appropriately. The scaling exercise is reasonably simple, while the removal of the steel ledges and the installation of blocks within the apparatus is already possible in the current design. It is also suggested that the tray moulds for the construction of the concrete blocks is outsourced to those more skilled in the trade. With the limited tools and expertise available, the similarity between supposedly identical moulds was not certain. This led to a significant amount of time being spent on sanding and grinding blocks to size. Fracturing of blocks was identified as a problem, but is very difficult to avoid. The introduction of softer supports may alleviate this problem, but, with the loads involved, it is expected that this will remain a problem.

The numerical modelling can also be improved and expanded upon in a number of areas. As noted above, the shear response of the rockbolts should be modelled. A shear model has been developed and will be implemented in the near future. The models also need to be optimised in terms of efficiency. Considerations for accurate contact resolution tend to greatly increase analysis times: the analysis time for the simulation of the lab test was approximately 60 hours.

It is also possible that modelling the hangingwall as a beam subjected primarily to vertical loads is not the best way to evaluate the stability of the beam. Stability is, after all, the tendency of a system to remain stable when subjected to a perturbation of some sort. In the case of the modelling performed so far, the perturbation is in the form of a vertical load. It is perhaps more accurately represented by changes in the vertical and horizontal loads, and by changes in the ratio of these loads. The effect of shaking can also be modelled.

Ultimately, the question asked by the mining industry is: will installation of short bolts allow for a larger gap between the face and the first row of permanent support? To answer this question, the stability of the hangingwall must be explicitly determined. While the current work, which has focused on the strength of the confined hangingwall beam, does give an indication of stability, the full excavation and support sequence should be modelled to determine the potential for falls-of-ground in the rockbolt-supported region between the face and first row of permanent support.

This report details the progress in Phase 1 of the project – to determine whether short tendons can have a beneficial effect on stope hangingwall stability. This has been shown to be the case, however, many factors influence the effectiveness of bolting. The next phase of the project will be to characterise and quantify the effect of these parameters.

Future outputs envisaged for this project are:

- Development of a modelling methodology based on stability criteria
    - Full-scale numerical models including excavation sequences and the introduction of permanent support should be analysed to determine the stress conditions around the excavation and the modelled hangingwall profile.
    - Criteria should be developed for quantifying “stability” of the hangingwall.
    - Models should be constructed for each of these criteria, for example, a model where the horizontal confinement is reduced. The confinement at which beam failure occurs would be used as a criterion.
    - The stability (made up of a number of values obtained from each criterion) of various hangingwall types are thereby determined.
    - The influence of bolts can then be determined in terms of the criteria.

- The support influence of different types of supports
    - Different types of bolts can be modelled quite easily, including friction stabilisers (Split Sets), fully grouted bars and end-anchors and yielding bolts.
    - The sensitivity of the system to numerical bolt parameters should be studied, including the relative stiffnesses of bolt, rockmass and bond, and the relative values of non-linear properties.
    - The effect of pre-tension should be investigated.

- Influence of rock mass parameters
    - The influence of various parameters on hangingwall stability with and without bolts should be evaluated.
    - These include bedding spacing, discontinuity spacing, discontinuity orientation, contact friction angles and the influence of cohesion

- A detailed investigation of dynamic effects
    - The full impact of a rockburst on the stope hangingwall can only be estimated, and is particularly difficult to relate to real seismic parameters in plane strain models.
    - A modelling methodology must be developed to fully model rockburst loading.
    - If possible, laboratory models should also be developed for this purpose.

- Quantification of parameters for different hangingwall types
    - Various bolting patterns, types and orientations should be employed in all of the generic hangingwall types.
    - Quantification of stability criteria will allow selection of the best bolting strategy for each hangingwall type.

- Case studies
    - A pilot study should be undertaken, preferably allowing comparison between a rockbolt-supported and unsupported panel in similar areas.
    - The criteria identified above should be used to asses the relative stability of both panels.
    - This is a particularly ambitious part of the research and must be conducted with full cooperation from the mine and with constant participation and commitment from staff involved in monitoring and running the operation.
    - Rockbolt installation procedures must be adhered to and the bolt installations checked by random sampling.
    - The case study should be modelled as far as is possible.

6. References

Acheampong, E. 2001 – 2002. Personal communication.

Adams, G.R., Jager, A.J. and Roering, C.. Investigation of rock fracture around deep-level gold mine stopes. *Proc. 22nd US Symp. Rock Mech.* Boston, M.I.T.

Brummer, R.K. 1987. *Fracturing and Deformation at the Edges of Tabular Gold Mining Excavations*. PhD Thesis submitted to the Rand Afrikaans University.

Brummer, R.K. & Rorke, A.J.. 1984. Mining induced fracturing around deep level gold mine stopes. COMRO report: project GR3F01, report no. 38/84.

Cook, N.G.W.. 1962. *A Study of Failure in the Rock Surrounding Underground Excavations.* PhD Thesis submitted to the University of the Witwatersrand.

Daehnke, A., Andersen, L.M., de Beer, D., Esterhuizen, E., Glisson, F.J., Grodner, M.W., Hagan, T.O., Jaku, J.S., Kuijpers, J.S., Kullman, D.H., Peake, A.V., Piper, P., Quaye, G.B., Reddy, N., Roberts, M.K.C., Schweitzer, J.K., Stewart, R.D., Wallmach, T.. 1998. Stope face support systems. Final Report GAP330. SIMRAC.

Daehnke, A., Acheampong, E., Reddy, N., Le Bron, K.B. and Haile, A.T.. 2000. Support technologies to cater for rockbursts and falls of ground in the immediate face area. Final Report GAP606. SIMRAC.

Fairhurst, C. & Cook, N.G.W.. 1966. The phenomenon of rock splitting parallel to the direction of maximum compression in the neighbourhood of a surface. *Proc. 1st Cong. of Int. Soc. Rock Mech.*. Lisbon.

Gay, N.C.. 1976. Fracture growth around openings in large blocks of rock subjected to uniaxial and biaxial compression. *Int. J. Rock Mech. and Min. Sci. and Geomech. Abstracts.* No 13.

Gay, N.C. & Jager, A.J.. 1986. The influence of geological features on problems of rock mechanics in Witwatersrand mines. In Anhaeusser, C.R. & Maske, S. (Eds.). 1986. Mineral Deposits of Southern Africa. Vol. 1. Geological Soc. S. Afr., Johannesburg, pp. 753-772.

Geyser, D.. 1999. Personal communication from GAP606 Report: Daehnke, et al. 2000.

Jager, A.J.. 2001 – 2002. Personal communication.

Jager, A.J. and Ryder, J.A.. 1999. *Handbook of Rock Engineering Practice for Tabular Hard Rock Mines*. SIMRAC. Johannesburg.

Kersten, R.W.O.. 1969. *Structural Analysis of Fractures around Underground Excavations on a Witwatersrand Gold Mine.* MSc Thesis submitted to the University of Pretoria.

Leeman, A.R.. 1958. Some underground observations relating to the extent of the fracture zone around excavations in some Central Rand mines. *J. S.A. Inst. of Mining and Metall.* No. 59.

McGarr, A.. 1971. Stable deformation of rock near deep-level tabular excavations. *Journal of Geophysical Research*. Vol. 76, no. 29. October, 1971.

Malan, D. F.. 1988. Mechanics for the induction of horizontal stress in the stope hangingwall. COMRO internal note.

Roberts, M.K.C.. 2001 - 2002. Personal communication.

Roering, C. 1978. Confidential COMRO report.

Roering, C. 1979. Confidential COMRO report.

Squelch, A. P.. 1990. Horizontal stresses in the face area hangingwall of backfilled and conventional stopes at Vaal Reefs. COMRO internal note.

Stillborg, B.. 1994. *Professional Users Handbook for Rock Bolting.* Trans Tech Publications. Sweden.

Thompson, A.G. & Windsor, C.R.. 1992. A classification system for reinforcement and its use in design. CSIRO Rock Mechanics Research Centre. Perth, Western Australia.

Van der Merwe, J.N.. 1998. *Practical Coal Mining Strata Control 2nd Ed*

7. Appendix

7.1. Testing of simulated Vaal Reefs hangingwall

These tests were performed before the laboratory testing described in the body of the report. As stated before, these tests were ultimately unsuccessful. Many lessons were learned as a result of this failure, which greatly assisted planning and construction of the other test set.

The principal is essentially the same as that described in section 3 – a bolted and unbolted model of a confined hangingwall beam subjected to vertical loading. There were some crucial differences between the tests though:

- Geometry
  - These tests modelled a generic Vaal Reefs hangingwall, with four layers spaced at 5 cm. The model is illustrated in Figure 55.
  - Shear and extension fractures were included in the model. The shear fractures penetrated to the top of the model and the extension fractures through the first two layers. Shear fractures were oriented at 110^0 and spaced at 15 cm. Extension fractures were oriented at 80^0 and spaced at 5 cm.
  - The in-plane length of each block was 45 cm, as opposed to the 22 cm in the subsequent tests. Many blocks broke upon removal from the moulds.
- Materials
  - Standard Conbextra AU concrete was used, cured for 23 days for the unbolted model, and 18 days for the bolted model.
  - 1 mm wire was used to model bolts. The bolts were “grouted” using Pratley putty, not epoxy.
- Procedure
  - Wooden dowels were used to create holes for bolts. Removal of these proved difficult and the holes did not always line up.
  - For the bolted model, the bottom two layers were cast together by combining two of the tray moulds. Construction, pouring and removal of blocks was extremely complicated and resulted in an irregular in-plan profile for these layers.
- Setup
  - No confinement was supplied parallel to the discontinuities (i.e. the hydraulic jack was absent).
  - The setup of platens resulted in the Vetter bag applying non-uniform loads. It was clear that the lowest layer was not adequately confined

Figure 55. Vaal Reefs laboratory model

The fact that in-plane confinement was omitted and that the lateral confinement was not fully applied to the lowest layer meant that the beam was not self-supporting. As soon as the supporting board was removed, the model fell down. The decision was made to support the beam with a soft foundation, which could prevent fallout while maintaining minimal resistance to displacement. A large block of polystyrene was used for this purpose. The test setup is illustrated in Figure 56.

This approach may have worked, given that the aim was to compare the bolted and unbolted result, however, the resistance offered by the polystyrene was much more than anticipated. The mistake was in supporting the entire area under the beam with the polystyrene. Over this large area, the resistance generated was enough to cause cracking of the concrete throughout the model. This reduced the hangingwall stability test to a test of combined concrete-and-polystyrene strength. Since the concrete in the unbolted model had cured for longer, the results indicated that the unbolted model was stronger than the bolted model. The load-displacement curves are presented in Figure 57.

The first lesson taken from this experience was to keep things simpler. The geometry of the subsequent lab tests was simpler – with only a single discontinuity set - and contained only two layers. The in-plane length of the blocks was halved. The blocks were therefore all intact upon extraction from the moulds. This also reduced the probability of cracking across the length of the blocks. The composition of the custom-made concrete also helped greatly. Not only was the curing time greatly reduced, but with a smaller aggregate size, the relatively small blocks were more robust. Bolt-holes were introduced with much greater efficiency. The steel nails were much easier to remove and produced clean holes which lined up very well.

The procedure was revised. It was determined that it was essential for the beam to stand up without support, hence the introduction of the in-plane confinement. The effectiveness of the Vetter bag in confining the lowest layer was also evaluated. Various platen configurations were tried before it was decided that both layers were being confined with comparable confidence.

While these tests were a failure and did cost over 100 hours (excluding curing time), the lessons learned allowed for a much more effective methodology to be developed.

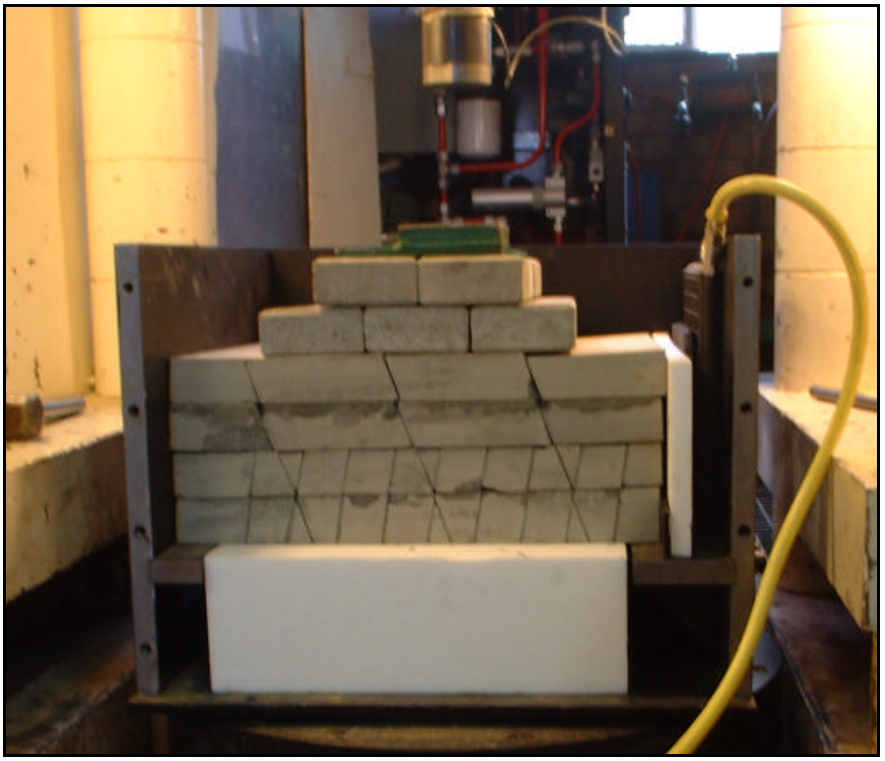

Figure 56. Test setup for the Vaal Reefs hangingwall model

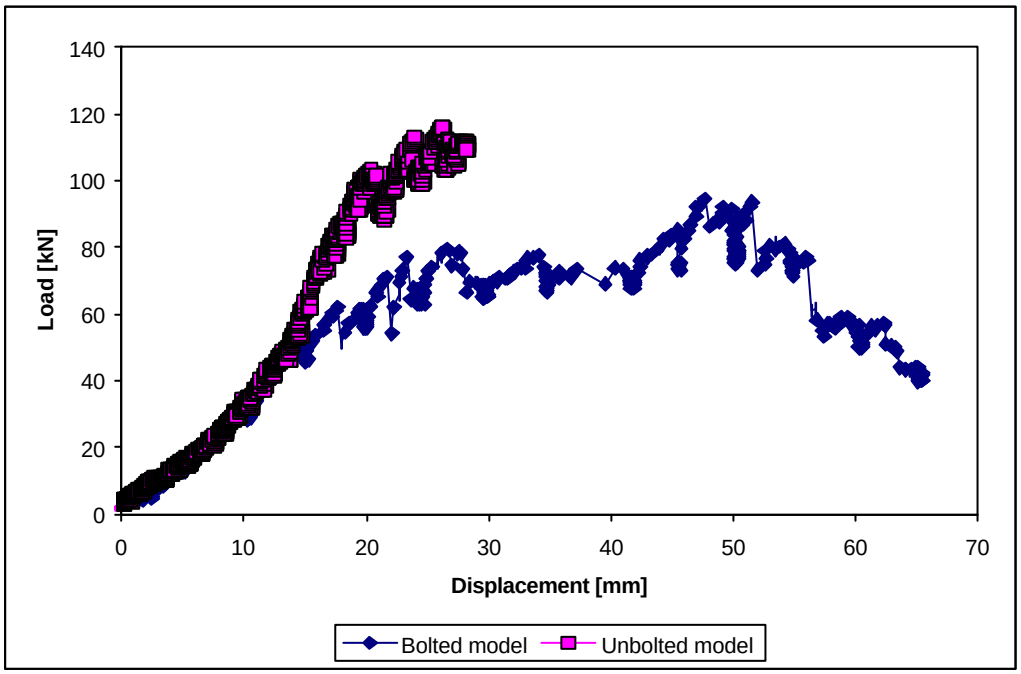

Figure 57. Load-displacement curves for the Vaal Reefs Laboratory models